DETERMINING THE ORBITAL ELEMENT AND ABSOLUTE MAGNITUDE DISTRIBUTION OF MAIN BELT ASTEROIDS

By

TIMOTHY BRUCE SPAHR

A DISSERTATION PRESENTED TO THE GRADUATE SCHOOL
OF THE UNIVERSITY OF FLORIDA IN PARTIAL FULFILLMENT
OF THE REQUIREMENTS FOR THE DEGREE OF
DOCTOR OF PHILOSOPHY

UNIVERSITY OF FLORIDA

1998

Dedicated to my parents.

ACKNOWLEDGEMENTS

There are too many people that have been essential to this work to acknowledge them all, but I will try to include the most instrumental. Brian Marsden has been continually supportive. Gareth Williams was always ready to provide ephemerides for new BSS objects, and it seemed he was always connected to a computer somewhere. Carolyn and Gene Shoemaker were always helpful, even after the Great Comet Crash had them circling the globe to attend meetings. Without Steve Larson's help, assistance, and support, there would have been no BSS. My friends Dave, Jo, Tony, Kirk and Nicole kept me sane by forcing me to play cards at least once a week. I thank my good friend and colleague, Carl Hergenrother, for putting up with me during long, tedious observing runs with the Schmidt. Finally I thank Joanna for her support, her enthusiasm, and her heart.

TABLE OF CONTENTS

ACKNOWLEDGEMENTS iii

ABSTRACT vi

CHAPTERS

1 INTRODUCTION 1

1.1 Reasons 1
1.2 History and Past Surveys 3
1.3 Orbital Elements 5
1.4 Structure of the Asteroid Belt 7
1.5 Contents 11

2 MDS, PLS AND SPACEWATCH 20

2.1 Starting Point: The McDonald Asteroid Survey 20
2.2 The Palomar-Leiden Asteroid Survey 21
2.3 Inclination Limitation of the PLS 22
2.4 The Problem with Forced Eccentricity 23
2.5 Is m_0 a Useful Quantity at all? 23
2.6 The Spacewatch Survey 24
2.7 PLS, Spacewatch, and the Cataloged Asteroid Population 25

3 THE BIGELOW SKY SURVEY 35

3.1 What is the BSS? Who Were the Main Players? 35
3.2 Background and Motivation 36
3.3 General Information 37
3.4 General Discussion 40

4 DEBIASING THE PLS 47

4.1 How Does Debiasing Work? 47
4.2 How to Calculate P? 48
4.3 The TBS Monte-Carlo Method for Detection Probabilities 49
4.4 How Does P Vary for a Standard Field? 51
4.5 Application to the PLS 52
4.6 Determination of the PLS *V* Magnitude Efficiency 52
4.7 Why the PLS Will Underestimate the True Numbers of Asteroids in Each *H* Bin. 53
4.8 The Trend with Longitude of Perihelion 54

4.9 Results 54
4.10 Additional 56

5 DEBIASING THE BSS 74

5.1 Introduction 74
5.2 Generated Objects and Detection Efficiency 75
5.3 Results 77
5.4 General Trends in the Region $a = 2.6$ - 3.3 AU 77
5.5 New Families 78

6 WHERE IS THE BEST PLACE TO LOOK FOR CERTAIN TYPES OF ASTEROIDS? 86

6.1 The General Concept 86
6.2 Quantitative Study: Eos and Maria Family Asteroids 86

7 SUMMARY 90

7.1 Conclusions 90
7.2 Future Work 92

REFERENCES 95

BIOGRAPHICAL SKETCH 97

Abstract of Dissertation Presented to the Graduate School
of the University of Florida in Partial Fulfillment of the
Requirements for the Degree of Doctor of Philosophy

DETERMINING THE ORBITAL ELEMENT AND ABSOLUTE MAGNITUDE DISTRIBUTION OF MAIN BELT ASTEROIDS

By

Timothy Bruce Spahr

May 1998

Chairman: Dr. Stanley Dermott
Major Department: Astronomy

We present here two general techniques to remove observational selection effects from asteroid surveys. When applied to two specific asteroid surveys, these methods have allowed the first computation of the debiased distribution of asteroidal orbital elements and sizes for the first time. The first survey was conducted in 1960. Advances in computing have allowed the data to be re-analyzed using an existing computer program and given a much more rigorous statistical treatment. The survey was confined to the near-ecliptic at opposition, therefore its usefulness is limited with regard to highly inclined orbits. To compensate for this limitation, we conducted our own survey aimed specifically at high-inclination objects. Since these orbits are, in general, distributed differently than lower-inclination orbits, removing observational selection effects required creating a statistical technique using Monte-Carlo type simulations.

The results of this work show no evidence for differing slopes of the size-frequency distribution throughout the asteroid belt, from the highly inclined Hungaria-type asteroids in the inner edge of the belt (1.8-2.0 AU), to the outer belt 3-3.5 AU). The slopes of the absolute-magnitude frequency distributions, being less than 0.5, show that the asteroidal size distribution is somewhat shallower than what would be predicted assuming the asteroids to be a collisionally evolved population of bodies with size-independent impact strengths. Also determined are rough numbers of asteroids in the main dynamical families of Eos, Maria, Themis, and Koronis, which comprise a significant fraction of the total number of objects in the main belt. This work has also resulted in the discovery of a new asteroid dynamical family, and possibly two new asteroid groups.

CHAPTER 1
INTRODUCTION

Scientists who wish to obtain useful statistical information on a large population of objects are faced with two choices: observe and catalog the entire population or observe some smaller sample of the whole and scale these data in some meaningful and appropriate fashion in order to obtain information about the whole. To extend the results of a small-scale survey to the whole population requires some *debiasing* technique to remove the observational selection effects. This is precisely the problem facing astronomers studying asteroids. It is estimated that there are at least 1,000,000 asteroids with diameters greater than about 1 km, yet the present detected population contains only about 50,000 members. There have been many surveys aimed specifically at discovering and cataloging asteroids over the past 50 years, but very few have attempted to remove observational selection effects and predict the total population of asteroids down to a given size. As a result, we have observational completeness on objects down to only about 25 km, or those objects with absolute magnitudes, H, less than about 11.0. (H is the V magnitude of the asteroid at the mythical location of 1 AU from both the Sun and the Earth at zero phase angle.) The aim of this work is to introduce two debiasing methods and apply them to two different asteroid surveys in order to obtain the best estimate for the distribution of main belt asteroid orbits and sizes for the first time.

1.1 Reasons

First and foremost, this Thesis is an attempt to gain a better understanding of the numerous observational selection effects that influence asteroid surveys.

While some general trends are already known, this subject is largely unexplored. By the conclusion of this research, we should have a solid understanding of the most important selection effects present in asteroid surveys.

Perhaps the most important reason for this work is to determine the mass-frequency distribution of the asteroids. The mass distribution is not obtained directly, but indirectly from the size distribution, or the absolute magnitude distribution. Dohnanyi (1969) found that the mass distribution of a set of mutually colliding bodies, all with size-independent impact strengths, could be described by:

$$f(m)dm \propto m^{-q}dm \tag{1.1}$$

with $f(m)$ being the number of objects in the mass range m to $m + dm$ and q, the slope index, $= 11/6$ for collisional equilibrium. To compare with the absolute magnitude distribution, i.e., a plot of $\log(n)$ versus H, with n being the incremental (and not the cumulative) number in a bin of H, the slopes are related by the following equation:

$$q = \frac{5}{3}\alpha + 1 \tag{1.2}$$

where α is the slope of the absolute magnitude-frequency distribution. In the case of collisional equilibrium, $\alpha = 0.5$ for objects with size independent impact strengths. An α value significantly different than 0.5, confirming the results of Durda and Dermott (1997), would place constraints on the strength-scaling law for asteroids and perhaps provide us with clues to asteroidal composition and structure. Unfortunately, our observationally complete set (the set of asteroids down to a certain size that we have discovered very nearly every existing member) only contains 2644 members and extends only to $H = 12.5$ in the inner belt, and $H = 11$ in the outer belt. Without debiasing the asteroid belt to $H > 13$, our observationally complete set will provide no information on α (and hence q) since the transition to the collisionally evolved portion of the asteroid belt occurs at $H \sim 13$ (see also Durda and Dermott 1997). With α, or q in hand, we will be able to predict the amount of dust in the Zodiacal Cloud from asteroids alone.

Another important result to be obtained from this work will be the total number of asteroids in the main families. This can in turn be used, along with q, to predict the amount of dust injected into the Zodiacal Cloud from these main families.

The orbital element distribution and number density, particularly for those objects near resonances, will allow us to get a direct estimate of the number of objects on unstable orbits, and thus an estimate of the number of objects required to replenish these areas. If the expected number of Near-Earth Objects (NEOs) from this type of analysis is too small, it will indicate a significant number of extinct comets exist in the NEO population.

High-inclination asteroids are always undersampled by ecliptic surveys. The absolute magnitude distribution of these objects will be of importance to determine whether or not the size distribution is different than that of other regions of the asteroid belt, as these high-inclination objects collide less frequently than other objects, but do so with much higher mean impact velocities. Because there are so few high inclination objects in the observationally complete set, a survey that presents the debiased orbital element distribution of these high-inclination objects wll be of use simply so that we can, for the first time, view the orbital element distribution of these objects.

1.2 History and Past Surveys

Surveying for asteroids has taken place on and off for nearly 200 years. In September 1800 the infamous "Celestial Police" met to discuss searching for the mythical missing planet between Mars and Jupiter. These 24 astronomers chose to divide the ecliptic in 15 degree swathes, and searched for the missing planet visually.

They expected the planet, like Uranus at discovery, to show a noticeable disk. Unfortunately for them, Piazzi discovered Ceres in January 1801, before the "Police" could even get out of the starting blocks. His method, which is essentially the same method used today to search for asteroids, was to look for motion with respect to the background stars. Three other bright asteroids were discovered in the next few years, but it was not until 1845 that the fifth asteroid was discovered. Most of the first few hundred asteroids were discovered, not by the Piazzi method, but by comparing given fields with star charts. Any object not listed on the star chart was returned to some time later to see if it had moved.

The photographic process revolutionized asteroid surveying. Wolf was the pioneer in this field, making the first photographic discovery of an asteroid in 1891. Wolf's method was simple enough: he looked for the trails left by asteroids during long exposures tracked at the sidereal rate. Wolf would expose two plates of each region, with the second plate verifying the discovery and giving the sense of motion. During the early 1900's, a new method for asteroid detection was used. Two plates of the same region of sky were taken on the same night and examined in a blink comparator. This device consisted of two separate optical systems that delivered images of exactly the same location on the two plates to a single eyepiece. A small kicker mirror allowed the user to flip back and forth between the plates rapidly, and objects moving with respect to the background stars "wiggled" or "blinked" and were easily detected. Tombaugh's discovery of Pluto in 1930 was in fact made with a blink comparator. Shoemaker in 1980 was the first to use stereoscopy to search for asteroids. This method is very similar to that of the blink comparator, but instead of having one eyepiece and a kicker mirror, the device has one eyepiece for each eye. A 3-dimensional image is created, and moving objects are detected because they appear to "float" or "sink" based upon their motion. This method was used with great success by Helin *et al.* and Shoemaker *et al.* (Carusi *et al.* 1994) during their very successful Near-Earth Object (NEO) surveys of the 1980's and 1990's. This method is also used in the Bigelow Sky Survey (BSS), which is discussed in detail in Chapter 3.

The advent of CCD technology has once again revolutionized the field of asteroid surveying. While CCD chips are still very small, and cover a small region of sky compared to a single plate or film, they nonetheless are quite efficient for surveying as they have a much higher quantum efficiency than photographic emulsion. In addition they require no time consuming detection processes such as blink or stereo comparing. Astrometry with CCDs takes only a scant few minutes, compared to hours in the case of photographic plates or film. The Spacewatch survey of Gehrels *et al.* (to be discussed in Chapter 2) (Carusi *et al.* 1994) was the first team to use CCD's exclusively for their asteroid surveying and, to date, this is the most effective NEO survey in history. Their method consists of taking 3 scans of the same region of sky a few minutes apart to look for moving objects. Their software shifts all three frames such that the background stars are in exactly the same location, and looks for objects that move between the frames. Other groups, mainly the Near-Earth Asteroid Tracking project, (NEAT) at JPL, a new European team named ODAS, a Chinese team at Xinglong, and an Air Force group from Lincoln Labs (LINEAR), are also using Spacewatch-type detection algorithms. In addition, numerous amateur astronomers are nowadays using CCD-equipped small telescopes for asteroid discovery and follow-up.

1.3 Orbital Elements

At any given instant, an asteroid orbit is defined by 6 quantities, namely the orbital elements of the instantaneous two-body orbit fitted to the asteroid's position and velocity. a is the semi-major axis of the ellipse; e is the eccentricity of the ellipse; and i is the inclination with respect to the ecliptic, which is the reference plane of the solar system. Ω is the longitude of the ascending node, and it is the angle between a specified reference direction, in this case the Vernal Equinox, and the location where the orbit punctures the ecliptic from below. ω is the argument of perihelion, which is the angle between the direction of perihelion and the line of nodes. ϖ, known as the longitude of perihelion, is simply the sum of ω and Ω. Because of perturbations of the planets, osculating orbits are continually changing by small amounts, and observations that require very precise locations (to the nearest arcminute) will require osculating element updates every $\sim$ 100 days. These planetary perturbations are broken up into 3 types: short-term, secular, and resonant. Short-term perturbations are those non-resonant perturbations that involve mean longitudes of the asteroid and the perturber, and are essentially random encounters. These will average out to zero, and for our purposes are ignored. Resonant perturbations are those which involve the mean longitudes, but are "repeating". In this case, the ratio of the mean motions or the average orbital period, n is:

$$\frac{n_1}{n_2} = \frac{p}{p+q} \tag{1.3}$$

where p and q are integers, and q is the "order" of the resonance. These perturbations are additive in the sense that a particular configuration of the two bodies will repeat every q orbits.

Secular perturbations are also called "slowly varying" or "long-term". These are independent of the mean longitudes of the bodies, and are dependent only on the orientation of the orbits themselves. The effect here is as if the perturber's orbit is represented by a ring of material, with the mass distributed in such a way that the total mass of the ring is the mass of the perturber, and the ring density is proportional to the amount of time the perturber spends at each point in its orbit. Secular terms result in the standard circle diagrams seen in Figure 1. The circle results from the sum of two vectors, one constant and one that varies with time. The free or proper component is indicative of the initial conditions of the asteroid, and the forced component is due mainly to the influence of Jupiter. As the orbit precesses, the proper component precesses around the circle, resulting in a varying osculating component, which is the vector sum of the forced and proper compontents. Because the circle is not centered on zero, asteroidal orbits tend on average to have higher osculating eccentricities than if there were no forcing, and the orbits tend to spend most of their time with a ϖ value near that of ϖ_{forced}, or that of Jupiter, as depicted in Figure 2. This bias, intrinsic to this particular dynamical system, is critical to our discussion of observational selection effects.

1.4 Structure of the Asteroid Belt

Our present understanding of the structure of the asteroid belt is limited by observational selection effects. We can, however, notice much of the overall structure by looking at only the brightest objects, or those objects for which we have observational completeness. As noted by Durda and Dermott (1997) and Jedicke and Metcalfe (1998), the main belt ($2.0 < a < 3.5$ AU) is surveyed nearly completely to absolute magnitude $H = 11.0$. This set contains 1449 objects with well-determined orbits. Jedicke's work does in fact present faint limits for the inner ($2.0 < a < 2.6$ AU), middle ($2.6 < a < 3.0$ AU) and outer ($3.0 < a < 3.5$ AU) regions as $H_{lim} =$ 12.75, 12.25, and 11.25, respectively, and there are 2644 objects in this set. When looking at osculating $a - i$ and $a - e$ plots for these objects (Figure 3 and Figure 4), much structure can be seen. Mean motion resonances, secular resonances, families, groups, and large voids are apparent. These are discussed in turn below.

Chaos. Much of the study of the dynamics and structure of the asteroid belt is now centered on the study of nonlinear dynamics and chaos. The vast majority of the objects we see in the main belt are stable over the lifetime of the solar system. Those that are on unstable, chaotic orbits are continually being removed by close encounters or collisions with planets (or the Sun) on timescales much less than the age of the solar system. This implies that there must be sources for objects that are on chaotic orbits.

Mean Motion Resonances. It is obvious in looking at Figures 3 and 4 that objects with a near 2.00 AU, 2.50 AU, 2.8 AU, and 3.25 AU are very rare. These regions correspond to the main mean-motion resonances with Jupiter. Kirkwood (1867) was the first to notice these empty regions. Objects that enter these chaotic regions of the belt can have their e values increased dramatically (Wisdom 1982) and will be ejected on timescales $\sim 10^7$ years due to collisions or close encounters with terrestrial planets, close encounters with Jupiter, or as has more recently been suggested, collisions with the sun. (Levison and Duncan 1994).

Librators. Along with depleted zones, there are also zones of enhancement in the asteroid belt due to resonance. The Trojan (1:1 resonance with Jupiter or $a =$ 5.2 AU) and Hilda (3:2 resonance with Jupiter or $a = 4.0$ AU) populations are also noted on Figure 3. While most of the Hilda population is in fact Jupiter-crossing, the objects are nonetheless protected from close encounters with Jupiter by the resonant nature of the orbit. These objects have their aphelia when Jupiter is on the opposite side of the Sun, and their perihelia are at safe distances of a few AU from Jupiter. So-called Trojan asteroids are in safe 1:1 resonance being centered around roughly ± 60 degrees heliocentric longitude from the primary. There are several hundred known Jupiter Trojans and to date two known Trojans of Mars. Jupiter Trojans have higher mean i than main belt asteroids, and this is expected due to either the presence of a secular resonance (see below), or the possibility that they are captured long-period comets (Shoemaker *et. al* 1989). The two known Mars Trojans have i of 20 and 19 degrees, respectively, although the high inclination in this case is expected because of the stable regions being associated with narrow and specific ranges in inclination space dubbed “inclination windows” (Mikkola and Innanen 1994).

In addition to the Hilda and Trojan populations, there are also a very few objects in the 2:1 resonance due to the same avoidance mechanism as that employed by the Hilda population. Asteroid (1362) Griqua, along with $\sim$ 5-10 other objects, is locked in permanent 2:1 resonance with Jupiter and avoids large perturbations by having its aphelion on the opposite side of the sun from Jupiter.

Secular resonances. Objects with $\dot{\varpi}$ or $\dot{\Omega}$ equal to that of one of the eigenfrequencies of the planetary system will also exhibit chaotic behavior. These are the secular resonances. The ν_6 resonance (associated primarily with $\dot{\varpi}$ of Saturn) has long been thought to be an efficient resonance for delivery of meteorites to Earth, and hence also responsible for many NEO's (Wetherill 1979). The ν_5 resonance (associated mostly with $\dot{\varpi}$ of Jupiter) appears at rather high inclination but is still effective in pumping up the e and i values of objects trapped there. The ν_{15} resonance (associated with $\dot{\Omega}$ of Jupiter) is thought to be responsible for some of the high-i Apollo asteroids. Figure 5 shows the location of the main mean-motion and secular resonances in a and i space. It should be noted that these secular resonances are surfaces in orbital element space, whereas mean motion resonances occur at only specific values of a and e.

Recently, Michele (1997) has shown that secular resonances with the terrestrial planets dominate the motion of NEO's with $a < 2$ AU. This important result shows how strong these resonances can be, and also points out that integrations of solar-system objects which do not include all of the planets are not reliable.

Regions of resonance overlap. There are several gaps in the asteroid belt that are nearly devoid of asteroids, notably the inner region near 2 AU from low to high inclinations, and the outer region beyond 3.25 AU at medium to high inclinations. These are areas with more than one resonance active, and objects here will be unstable on very short timescales. The region near 2.0 AU between the Hungaria and Phocaea populations in inclination is home to 4 resonances! This area is nearly completely clean of asteroids to date, and those that are present seem to be in transition to NEO's (eg, 1997 AB_{15}, $a = 2.05$, $e = 0.38$, $i = 38$). Mars itself probably plays a role in sweeping this area clean, since even low e values will produce chaotic planet-crossing orbits, and the effect of these resonances is to increase e.

Asteroid families. Hirayama (1918) noticed, while looking at diagrams similar to those in Figure 1 that some asteroids seemed to have very similar proper elements. These are the asteroid families. While families can be discovered by looking at plots of osculating orbital elements, most families are noticed by comparing tables of proper elements. Proper elements are defined by Valsecchi *et al.* (1989) as "constants of integration of the differential equations of variation of orbital elements." In short, proper elements are osculating elements that have been corrected for the perturbations of the major planets (Gradie *et. al* 1979). The most populous asteroid families are (221) Eos, (24) Themis, (158) Koronis, and (170) Maria. Figure 6 shows the main belt in proper element space. All asteroid families are the collisional remnants of a series of catastrophic collisions that fragmented asteroids.

Asteroid groups. Groups are a different entity than families, although most groups actually do contain families. Common groups include Hungaria, Phocaea, and Pallas. These are dynamically isolated regions of the asteroid belt, and are not the result of the disruption of a large parent body as in the case of families. Inspection of Figure 3 shows that the region occupied by the Hungaria population ($a \sim 1.9$, $i \sim 23$) is bounded on most sides by resonances. The outer boundary (near $a = 2$ AU) is associated with the 4:1 mean-motion resonance with Jupiter and the ν_{16}, and the ν_6 secular resonances. At high inclinations, the Hungarias are cut off by the ν_5 resonance. The inner boundary in a, and outer boundary in e are probably swept clean by repeated encounters with Mars (aphelion $Q = 1.69$ AU). The Phocaea ($a \sim 2.3$ AU, $i \sim 25$ degrees) and Pallas ($a \sim 2.7$ AU, $i \sim 34$ degrees) groups are similar isolated regions, truncated by different combinations of secular and mean-motion resonances. Figure 6 labels the main groups and families on the a-i plot.

1.5 Contents

In 1950, Kuiper et al. (1958) undertook a massive observational program, the McDonald Asteroid Survey (MDS), specifically aimed at determining the statistics of brighter asteroids. To extend their results to the entire asteroid belt they attempted some simple bias corrections based on "mean" brightnesses of asteroids and logarithmic correction factors. The preliminary results indicated differences in the size distribution of different regions of the belt, so the authors undertook a second massive survey, this time aimed at the statistics of fainter asteroids. This was the now-famous PLS (Palomar-Leiden Survey) (Van Houten *et. al* 1970). As it will be shown, the debiased PLS and MDS do not predict accurately the number of now-known asteroids. Jedicke and Metcalfe (1998) made another attempt at debiasing a main belt asteroid survey. They created a model-independent technique for removing observational bias from an asteroid survey and applied it to data obtained during the Spacewatch survey. While their debiased distribution for H is probably very close to reality, their orbit distribution is suspect. These surveys, as well as the present cataloged asteroid population, will be discussed in detail in Chapter 2.

Both the PLS and the MDS were confined to the near-ecliptic regions, and consequently the results are very limited at $i > 15$ degrees. To properly debias the high-inclination asteroid population, we were required to design, conduct and debias a survey of our own specifically aimed at detecting these objects. We did just this with the Bigelow Sky Survey (BSS), which is discussed in Chapter 3.

Both the MDS and PLS used rather crude methods to debias their observational data. In Chapter 4 we investigate a general analytical method —the Jedicke method— of debiasing any particular asteroid survey. We will verify Jedicke's method by creating our own method to correct for observational bias using a Monte-Carlo simulation, and then apply a combination of both methods to the PLS. The results of this work will allow determination of the ratio of asteroids in the 4 main asteroid families (Eos, Themis, Koronis, and Maria) to that of all asteroids in the main belt. Also, a determination of the slope of the absolute magnitude-frequency distribution, α, is presented from this data, and this is translated to a mass index, q. Chapter 5 will use the Monte-Carlo method to debias the BSS, and again the debiased results present α and q values. These values are then compared to those determined in Chapter 4. The first determination of the orbital element distribution of these high-inclination objects is also presented here.

In Chapter 6 we will briefly discuss a method of selecting a specific area of sky to look for specific types of asteroids, and note that this area is not always in the ecliptic at opposition. In Chapter 7 we conclude by discussing the pros and cons of both debiasing methods, making some suggestions for future work on the subject, as well as the direction future asteroid surveys should take.

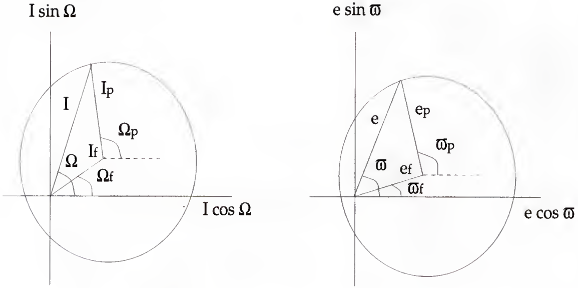

Figure 1. The relationship between forced and proper elements.

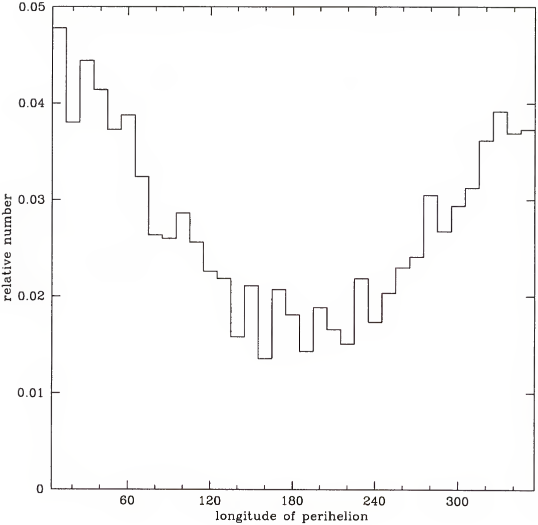

Figure 2. Trend in ϖ for the observationally complete set.

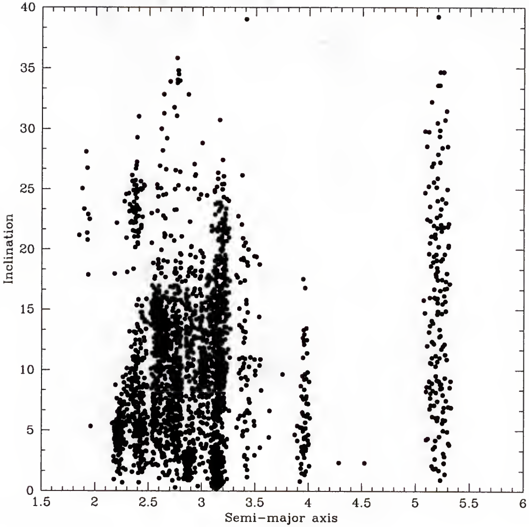

Figure 3. a and i for the observationally complete set.

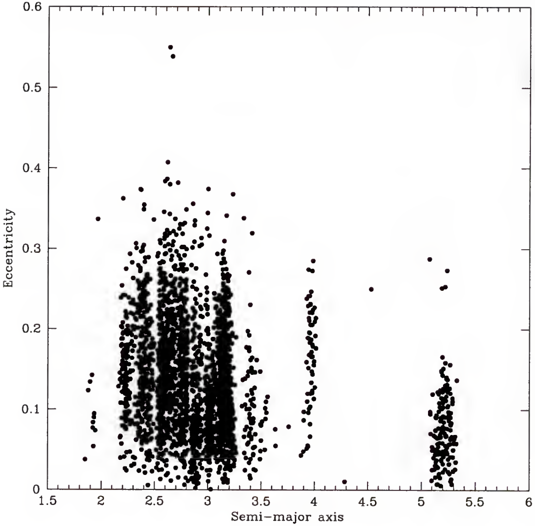

Figure 4. a and e for the observationally complete set.

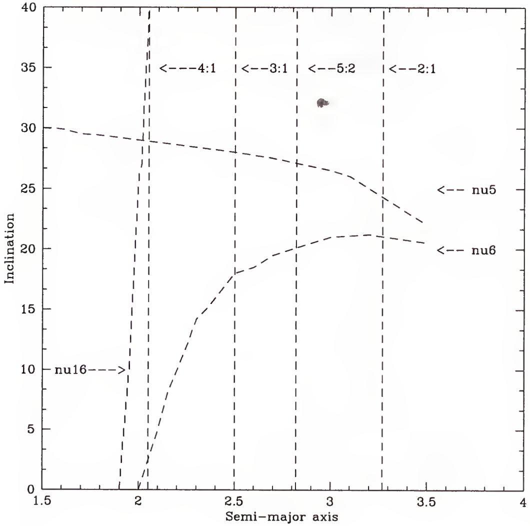

Figure 5. Location of the main resonances in the asteroid belt.

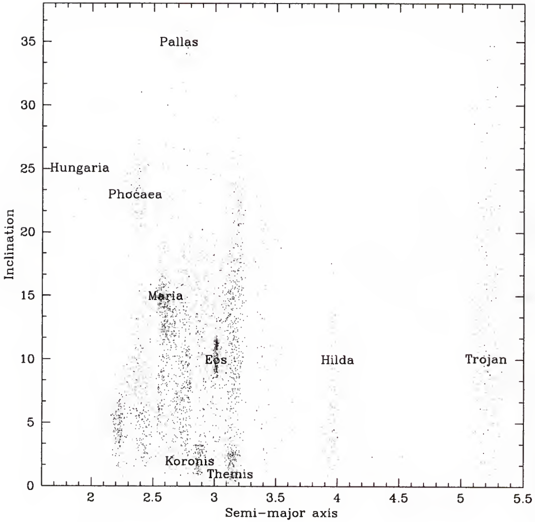

Figure 6. Location of the main groups and families in the asteroid belt.

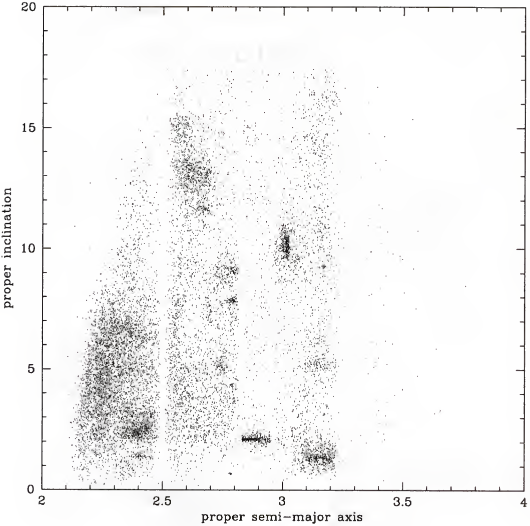

Figure 7. Proper a and i for asteroids.

CHAPTER 2
MDS, PLS AND SPACEWATCH

2.1 Starting Point: The McDonald Asteroid Survey

The MDS (Kuiper *et. al* 1958) is the starting point for any discussion of debiasing the asteroid belt. Conducted in 1950-1952, this survey used a 25cm f/7 wide-field telescope. Fields 6.5°× 8.1° were shot at one-hour intervals and examined in a blink comparator to search for moving objects. MDS chose to track on the mean rate for main-belt asteroids, and the effective plate limit was V magnitude 15.7. The aim of the MDS was to find the number of objects down to a certain limiting mean opposition magnitude, and correct the mean opposition magnitude formulae to absolute magnitudes. The mean opposition magnitude, m_0, is defined by the following equation:

$$m_0 = H + 5log(a(a-1)) \tag{2.1}$$

Here, a is the semi-major axis of the asteroid, and H is the absolute magnitude. m_0 is supposed to represent a rough average magnitude of an asteroid at any given time during its orbit. The term $a(a\text{-}1)$ is roughly equivalent to the geocentric distance of the asteroid, as the distance from the Sun to the asteroid is roughly a, and the Sun to the Earth is 1 AU.

To extend their results to the entire asteroid belt, the MDS authors computed a least-squares solution to the logarithm of the number of objects observed as a function of m_0, and reduced it to one "strip" of their survey in declination. To predict the total number of objects in the belt, they assumed that by scaling this strip to the entire sky, they could predict the number of asteroids as a function of m_0 in the entire sky. Simple logarithmic correction values were added or subtracted from their equation for m_0 to achieve this. For example, the addition of log(360/6.5) takes into account that the MDS strips in declination were only 6.5 degrees wide in Right Ascension. Following several such corrections, including those taking into account the ecliptic latitude limit of the survey and the overlap between strips, a formula was then presented that listed the number of asteroids as a function of m_0, over the whole sky. With a simple conversion from m_0 to H, and using the observed a distribution, we could then compare the number of asteroids as a function of H, averaged over the entire belt. Admittedly, this analysis was not presented at all clearly in their paper.

2.2 The Palomar-Leiden Asteroid Survey

After the analysis of the MDS was completed, the results indicated different α values for the three regions of the main belt, so the authors decided to undertake a second massive survey to determine the statistics of the fainter asteroids. Rather than cover all the way around the ecliptic, they chose to conduct a small-scale search and attempt to scale these results to the whole sky. In hindsight, one can see that this will have only limited usefulness due to many the complicating factors, but this survey has been the only attempt at debiasing the asteroid belt to fainter magnitudes. The Palomar-Leiden Survey (PLS, Van Houten *et al.* 1970) used the Palomar 1.2m f/2 Schmidt and concentrated on an area 18 degrees long by 12 degrees high, centered on the vernal equinox. These fields were shot several times in September 1960. The telescope was again tracked at the mean rate of main-belt asteroids and the effective faint limit was about 20 in V. The fields were shifted 6 degrees to the west to compensate for the average monthly motion of a main belt asteroid, and re-shot in October 1960, to allow 30+ day arcs on most of the objects discovered.

The PLS used essentially the same method that the MDS used for bias corrections, although there were slight differences because the area of sky covered was smaller. To deal with the inclination limitation of their data, the PLS used an approach based on the time spent within ± 5.9 degrees ecliptic latitude (β), which is the extent of their field, for an object in a circular orbit. This method will of course fail pretty miserably for objects with any significant eccentricity, which most main belt objects do indeed exhibit. Nonetheless, the correction was applied to all of their data. In addition, only objects observed during both months were to be used for statistics. This ensured that they would only consider objects with well determined orbits.

2.3 Inclination Limitation of the PLS

Both the MDS and PLS suffer with regards to incompletenss for high inclination asteroids. While the MDS attempted to cover ± 20 degrees in β each month, the PLS was restricted to ± 6 degrees in β. This restriction, as well as the stipulation that the objects be recovered the following month, severely limits the usefulness of this survey for high inclination objects. Most high inclination objects have large ecliptic latitude rates, and they will seldom remain within 6 degrees of the ecliptic for more than a month. Figure 8 shows the inclination distribution (without incompleteness corrections) of the PLS September detections, and Figure 9 shows the same for a PLS-type survey with a synthetic asteroid population similar to that of the main belt, but with inclinations random from 0 to 90 degrees. Because of the similar appearance of these plots beyond 15 degrees and the low relative number ($\sim$ 2%), we expect the PLS to be useful only up to $\sim$ 20 degrees in inclination. In further support of this contention, we note that while the PLS discovered 9 Hungaria-type asteroids (mean a, e, i = 1.92, 0.07, 22), they found zero Phocaea-type asteroids (2.35, 0.23, 23). Phocaeas and Hungarias have very similar motions and traces in β and ecliptic longitude (λ), and one would expect them to be discovered at a similar rate, all other things being equal. In addition, we will show in the discussion of BSS statistics (in Chapter 5) that there are actually more Phocaeas than Hungarias by at least a factor of 2 in each absolute magnitude bin. This makes the point more solid that the PLS data is positively not useful for $i > 20$.

2.4 The Problem with Forced Eccentricity

Another problem concerning the PLS bias corrections is that of the forced eccentricity. As seen in the Introduction, asteroidal orbits are configured such that they tend to line up their longitudes of perihelia with the longitude of perihelion of Jupiter (Kresak and Klacka 1989, see also Brouwer and Clemence 1961), and these objects have higher osculating eccentricities. Unfortunately, the PLS was conducted precisely when this effect would be the strongest. One would then expect the osculating eccentricities to be the highest for the PLS objects (at least those detected near perihelion) and that there would be 2-3 times as many objects discovered near perihelion during this survey than during a survey conducted at opposition 6 months later. PLS had no way of taking this into account with their bias corrections.

2.5 Is m_0 a Useful Quantity at all?

Both the MDS and the PLS used m_0 as the main factor for use in scaling their results to the whole asteroid belt. Since m_0 is supposed to represent the "average" magnitude of an asteroid, one immediately asks the question: Is this a representative quantity? Upon investigation, such appears not to be the case. After running several simulations, it is found that in almost all cases the actual magnitude of a given asteroid is 0.5-1.5 magnitudes fainter than m_0, presumably because there is no phase angle dependence in the equation for m_0, and because asteroids tend to spend more time at heliocentric distances larger than m_0. Taken at face value, this indicates errors of at least a factor of two in those surveys' scaling. It is also found that assuming m_0 to be representative of the average magnitude of an asteroid is worst for circular orbits. Since the mean orbital eccentricity is fairly low (~ 0.15), we can expect quite large scaling errors in all of the PLS data. PLS attempted to shift their data by +0.5 magnitudes to compensate for this, but they still underestimated the number of objects in each bin of m_0. The fact that this shift must take place at all indicates that this is most likely not a good quantity to use for scaling.

This form of debiasing also uses a somewhat dangerous method to tackle some difficult problems. Because the main equation used in the MDS and PLS is only a function of m_0, and not a physical quantity (such as a or e), the authors relied on the observed distribution of a in the three zones of a (2.0-2.6 AU, 2.6-3.0, and 3.0-3.5 AU) for the conversion between m_0 and H. The danger lies in using an unknown observable quantity, in this case the distribution of a in the main belt, as a scaling parameter. Strictly speaking, observed H and a distributions will be coupled; PLS will see fewer large a, large H objects because they are further away and fainter. Figure 10 and 11 from this chapter shows this. While the known population consists of many small a objects ($a \sim 2.2$ AU), the unbiased plot, Figure 10, shows that there are probably at least twice as many objects in the range $a \sim 3$ AU. This is a simple consequence of the fact that there are more intrinsically faint objects than intrinsically bright objects in the asteroid belt, and the faint objects are easier to detect when they are closer to the Earth.

2.6 The Spacewatch Survey

Since about 1985, Spacewatch at the University of Arizona has been conducting a NEO survey with a CCD-equipped 36" Newtonian telescope. Asteroids are detected by motion after three scans of the sky are taken. Spacewatch routinely detects several hundred new asteroids each night. A very recent advancement by two former Spacewatch employees, Jedicke and Metcalfe (1998), has allowed the first serious attempt at properly debiasing an asteroid survey. They applied their analytical method to data obtained during the Spacewatch survey. This method assumes that the angular orbital elements ω and Ω, as well as M, are distributed randomly, and computes $P(a,e,i,H)$, the detection probability, given that they know the field size and center as well as the V magnitude detection efficiency and the rate of motion efficiency. This has produced to date the best estimate for the orbit and size distribution of main belt asteroids. Unfortunately, Jedicke and Metcalfe applied their method only to objects that were detected on one night. This precludes any useful orbit determination, although it does allow the distance to be estimated, and hence the H distribution to be computed. Jedicke and Metcalfe present the a and i distributions, but their method is applied to the circular orbits they computed, and thus no e distribution is presented. Systematic errors in the a determination for high-i objects make their method particularly difficult to interpret for these objects. Figure 2 of their paper shows only 5 Phocaea asteroids detected in several thousand square degrees, but many more should have been detected. In addition, Jedicke and Metcalfe plot total numbers rather than normalized numbers of asteroids in the various bins. The effect of this is to bias once again toward the inner belt objects, since these objects are debiased to $H = 17$, and middle and outer belt objects are only debiased to $H = 16.5$ and 16.

2.7 PLS, Spacewatch, and the Cataloged Asteroid Population

The authors of PLS and Spacewatch papers have made predictions of the total number of asteroids in the main belt range 2-3.5 AU. These are compared with actual numbers of known objects in the three zones in Figure 5 from Jedicke and Metcalfe. (Figure 38 from this Thesis is a similar diagram.) The solid histogram is for known objects, bold points with error bars are the Spacewatch predictions, and the lighter points with error bars are PLS predictions. Note the roll off at fainter H values for the detected populations, and how the Spacewatch prediction matches the known population to the author's quoted completeness limits, while the PLS gives underestimates of the number of known objects in these ranges. Also included, in Figures 10-15 are a, e, and i distributions for all objects, $H < 16$, and the observationally complete sets. The dramatic difference in Figures 10 and 11 as well as more subtle differences in the remaining figures shows the level of bias in our total set of asteroids as compared to the observationally complete set.

It would seem, based on their Figure 5, Jedicke and Metcalfe's predictions are by far the best estimates of main belt asteroid orbits and sizes to date. But the most damaging argument against Jedicke and Metcalfe is the quality of the orbits they are using. In addition, there are obviously serious problems with the high-inclination asteroid populations. While this past work has added to our understanding of the statistics of main-belt asteroids, the need for both a properly debiased main belt survey using a, e, i, and H and a properly debiased survey specifically aimed at high inclination objects is obvious.

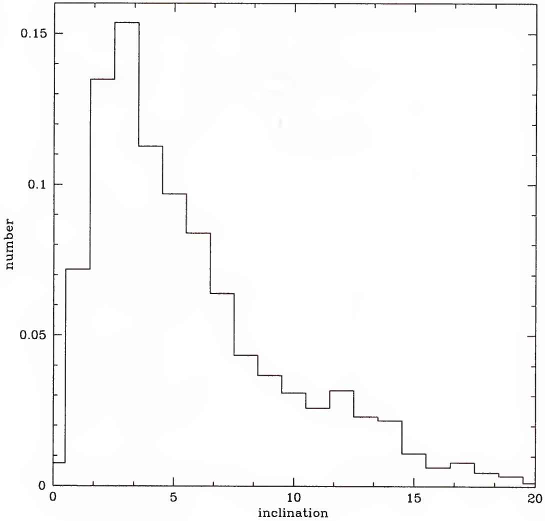

Figure 8. Histogram of inclinations for PLS September detections.

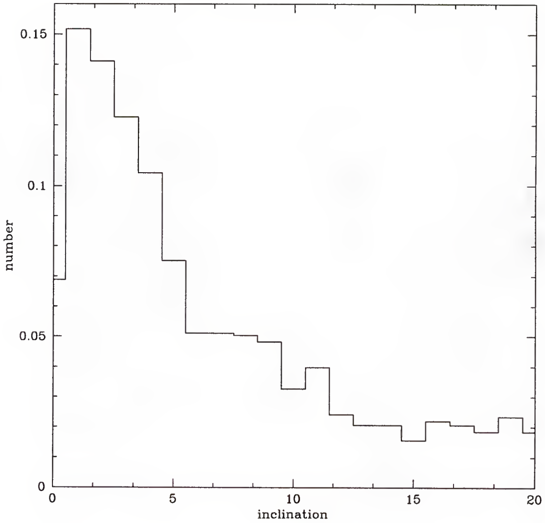

Figure 9. Histogram of incinations for a PLS-type survey, but with a simulated population of asteroids with random inclinations from 0 to 90 degrees.

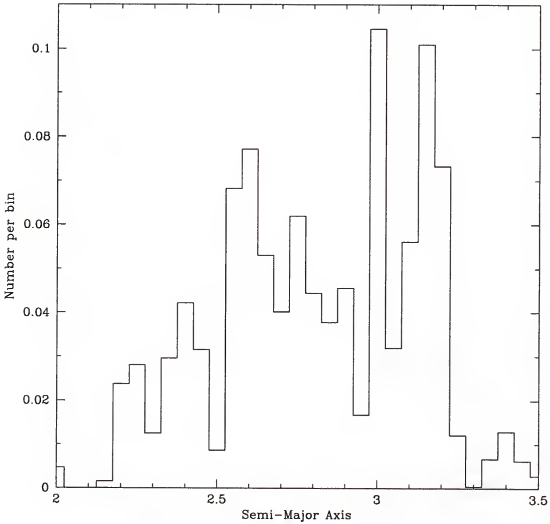

Figure 10. Histogram of semi-major axes for the observationally complet set as defined in the text.

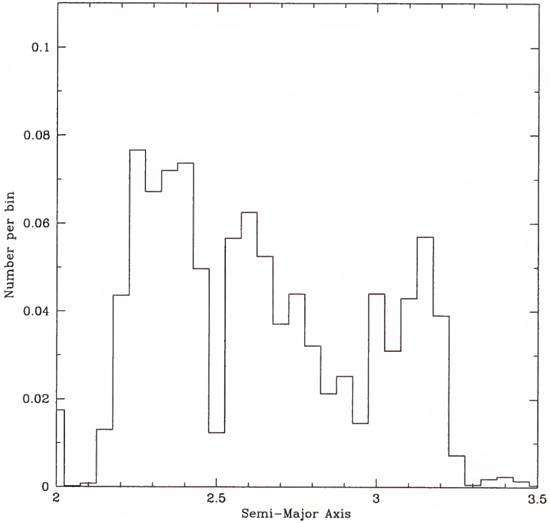

Figure 11. Histogram of semi-major axes for all objects with $H < 16.0$

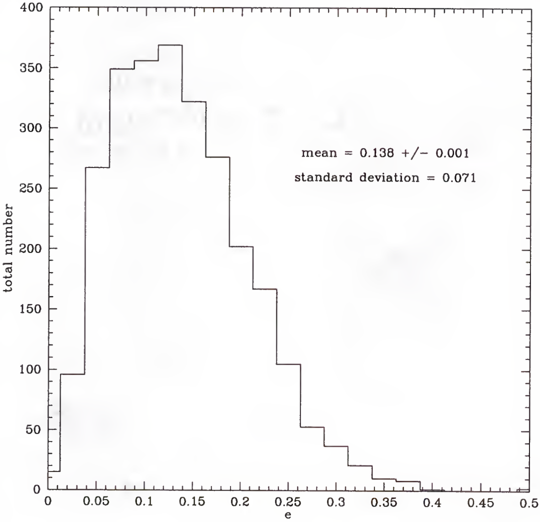

Figure 12. Histogram of eccentricities for the observationally complete set as defined in the text.

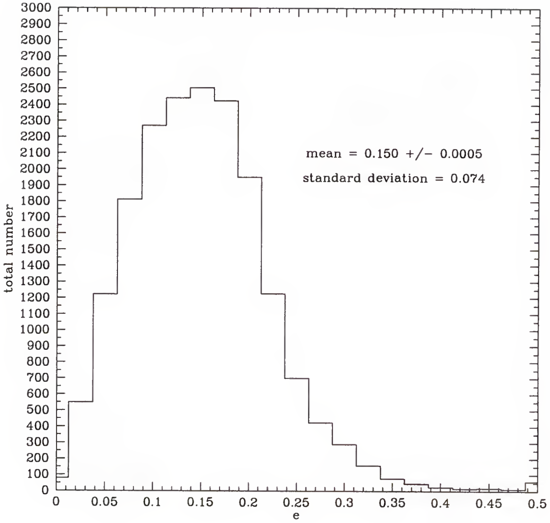

Figure 13. Histogram eccentricities for all objects with $H < 16.0$

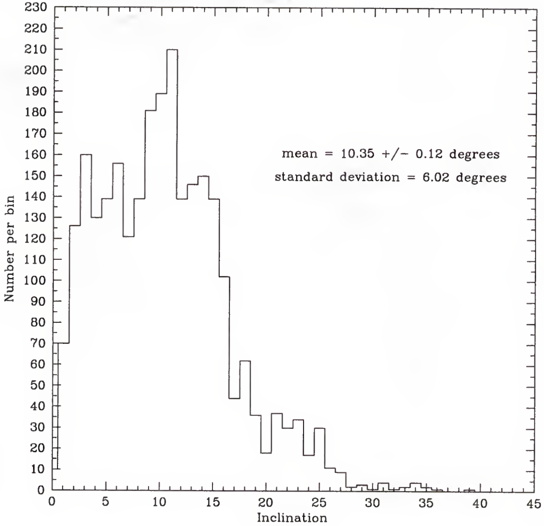

Figure 14. Histogram inclinations for the observationally complete set as defined in the text.

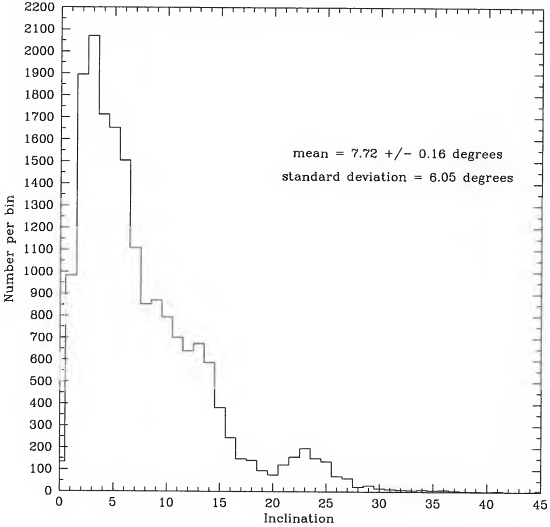

Figure 15. Histogram inclinations for all objects with $H < 16.0$

CHAPTER 3
THE BIGELOW SKY SURVEY

3.1 What is the BSS? Who Were the Main Players?

BSS stands for "Bigelow Sky Survey". Mt. Bigelow is the nearest major landmark to the Catalina Station of Steward Observatory, in the Santa Catalina Mountains northeast of Tucson, Arizona. This observing site contains a 61" reflector and the 16 3/4 inch Schmidt camera that was used to take all of the films for the BSS. The vast majority of the observing load was shouldered by myself and Carl. W. Hergenrother, who at the time was an undergraduate at the University of Arizona. Carl and I also shared all of the film scanning, with discoveries split roughly 2/3 to me and 1/3 to him, based solely on the fact that I scanned 2/3 of the films. For several key observing runs I was observing alone, hence the disparity in discoveries and films scanned. Other occasional observers were S. M. Larson, G. Esquerdo, R. Jedicke, and J. Brownlee. Larson is largely responsible for starting the survey, originally encouraging some tests, and providing film, the stereo microscope, and plenty of helpful suggestions and motivation.

It would not be proper to discuss the BSS without discussing the support of other people who were critical to the success of this survey. BSS is indebted to several amateur and professional astronomers around the world for providing critical astrometric follow-up observations. These include G. Viscome, D. Balam, J. Africano at the Air Force Maui Optical Station (AMOS), W. Offutt, R. McNaught, J. Child, A. Boatini, the observing crew at Klet observatory in the Czech republic including M. Tichy, as well as many other casual observers. This work was absolutely essential for recovery of lost objects and good orbit determination. Without these people BSS would not have succeeded.

3.2 Background and Motivation

Because high-inclination asteroids spend less time at low β than at high β, they have consistently been undersampled in all main-belt surveys. In order to present a complete debiased picture of the asteroid belt, the statistics of these objects must be considered. Given the option of finding 400 asteroids per plate on the ecliptic or 5 on a plate at 35 degrees β, nearly everyone chose to survey the ecliptic. High yield surveys, like the MDS and PLS for the main belt, as well as the NEO surveys conducted by Shoemaker and Helin (PACS and PCAS, respectively) with the Palomar 18" Schmidt, have contributed immensely to our knowledge of the NEO and main belt populations. While Shoemaker and Helin did not measure astrometrically all of the asteroids they detected, they did attempt to measure all of the unknown asteroids with "unusual" motion. High-inclination inner-belt objects like Phocaeas and Hungarias have larger apparent motion vectors than standard main-belt objects, and thus they were selected for measurement more often. But the simple fact that these surveys are inefficient for high inclination objects cannot be avoided. Also, considering the fact that debiasing will be totally impossible for PACS and PCAS (we have no idea of their efficiencies, exactly what field was covered, how many times, etc), we were forced to undertake our own survey for these high-inclination objects.

With the exception of Schmadel *et al.* (1989), there have not been any high-latitude surveys other than the BSS. They conducted a "foul-weather" survey for high inclination Hilda and Thule asteroids during 1977 with the ESO 1.2m Schmidt. This survey was conducted at latitudes -30 to -60 degrees during times of bad seeing and haze, when other "more important" projects that required photometric conditions could not be undertaken. They found a smattering of Hungarias and Pallas-type objects, but no attempt at debiasing was made. Of passing interest is their discovery of 1977 TD, an object independently found at Catalina by Hergenrother during May 1996. The object was hopelessly lost at the time of rediscovery.

BSS was originally designed to detect comets. Since long period comets have random inclinations from 0 to 180 degrees, we expected that a good many bright comets were being missed because of the incomplete coverage in β. After consulting Jim Scotti of Spacewatch and the Shoemakers, it was found that a high latitude survey would also compliment the existing photographic NEO surveys that terminated at around 30 degrees β. In March 1993, BSS began observing near the opposition meridian at 35 degrees β and working up in latitude from there. As luck would have it, the first field ever shot and scanned as part of the BSS contained a new asteroid discovery, 1993 EL.

3.3 General Information

BSS used the University of Arizona's Catalina Schmidt, located at elevation 2500m in the Santa Catalina mountains, some 30 miles northeast of Tucson. The telescope has a 16" 3/4 plate and a 28" diameter primary mirror, cut from a 48" sphere, resulting in a fast f/3 optical system. The platescale is about 170 arcseconds per millimeter, and with a circular cardboard mask 3.15 inches in radius, each field covered about 30 square degrees. While there were two plateholders that fit in the telescope, only one provided good enough focus to be used. It was loaded directly into the focal plane by means of a small hatch on the main telescope tube. After each exposure, the exposed film was removed from the plateholder, stored in a light-tight box, a new film was loaded into the plateholder, the plateholder loaded back in the telescope, and the telescope was slewed to the next field. This procedure required slewing the telescope from the horizontal to the proper field between each exposure. Average changeover time was around 5 minutes and 30 seconds, or nearly 70 % of the nominal 8 minute exposure time. Manual guiding was accomplished by centering a guide star in the field of view of the 8" f/12 refracting guide telescope.

While the telescope's nominal guiding was exceptional, corrections to the tracking were nonetheless required on 15-30 second timescales. Special care was taken to reposition the telescope properly (the telescope was still being pointed by means of setting circles) and to shoot the same guide stars on each film pair. Quite often this required "star-hopping" with the Uranometria 2000.

Some general tests were needed to determine which film was best for our needs. Ten-minute exposures of SA 68 (Everhart 1984) were taken on the same night using Kodak TMAX-400, TMAX-100, and hypersensitized Kodak Technical Pan 4415 films. (Hypering is a proces in which nearly all water is removed from the films or plates, usually by baking at near 150 ° C in a mixiture of nitrogen and hydrogen.) The faint limit using the TMAX-400 film was around V magnitude 18.0, which was much deeper than either of the other two films tested. Further experiments indicated that hypering TMAX-400 would allow us to go slightly fainter than 18.0 V, but the hypering process was very time-consuming, and quite inconsistent. For these reasons, as well as the fact that films had to be hypered in Tucson and carried to the mountain in a nitrogen-filled box (to prevent the films from losing the sensitivity gained by hypering), we decided to abandon the hypering process for the survey films.

Originally the films were developed for 12 minutes at 68 ° C in D-76 developer, this being the recommended time and temperature for nominal contrast. As luck would have it, an accident allowed a set of standard exposures of SA 68 to be developed at 80 ° for 12 minutes. These went much fainter and had greatly increased contrast than the previous films, and as a result we chose to adopt this development time and temperature for our standard exposures. These standard 8-minute exposures generally allowed the detection of asteroids moving at main belt rates to V magnitude 17.0-17.5. A few exceptionally faint objects were discovered during supreme conditions during September 1995, notably 1995 SS and 1995 SA_1 at V magnitude 18.2.

Guide stars were chosen at 30-50 degrees β at 5 degree intervals in both latitude and longitude for 265 fields total around the sky. Each field was shot twice per night with a preferred interval of 30 minutes. The area directly at opposition was the focus, although films were generally shot at ± 30 degrees from opposition in longitude. Films were scanned stereoscopically, using a device constructed by Steve Larson from spare parts, including the remains of the site for the main gun of a tank. A total of 609 fields were shot and examined from March 1993 through December 1996, resulting in 255 independent detections of 189 different asteroids; 71 were new discoveries, 15 objects were lost at the time of detection. 19 of the BSS detections were Mars-crossing asteroids (perihelion $q < 1.69$ AU), and 5 of these were NEO's, interestingly enough all Apollos ($q < 1.0$ AU). Table 1 lists the observing dates, number of fields exposed, discoveries and total area covered per observing run. Candidate objects not identified with known objects that had well-computed multi-opposition orbits were measured astrometrically by several means. Originally, this was accomplished by placing the films on a two-axis measuring engine, and measuring precise x-y locations of both the object and at least 7 Hubble Guide Star Catalog stars in both the zero and 180 degree positions. Because of the standard distortion associated with Schmidt optical systems, a parabolic fit was usually needed for sub-arcsecond astrometry. After a year or so of this type of astrometry, we changed to using a small video-rate CCD to digitize the area of film containing the object and the reference stars. Reductions were then completed using the Image Reduction and Analysis Facility (IRAF). In addition, an automatic star-matching and astrometry program was written by Tim Debenedictus for use during the Shoemaker survey, and we used this as well. Preliminary orbits were computed by either Brian Marsden or Gareth Williams of the Minor Planet Center (MPC) based on observations over an arc of more than three nights. Additional observations over subsequent months allowed general perturbed orbit solutions, and allowed many of the objects to be easily recovered at following oppositions. At present, a total of 18 BSS discoveries have orbits of sufficient accuracy (usually a runoff of less than 10 arcseconds per decade) that they have permanent numbers assigned by the MPC.

Precise magnitudes for each object were originally determined from simple visual comparison with Everhart's (1984) Selected Areas # 57 and 68. As a check, the magnitude for each detected object was also determined again by visual comparison using a set of B magnitude standards from the USNO A1.0 catalog. In general, BSS original H values were consistent to within ± 0.4 magnitudes. The cataloged magnitudes for most of the other detections were, in a word, atrocious. In particular, those determined by Helin *et al.* generally required a correction of +1. This sort of error is precisely why a systematic photometric survey of minor planets is very sorely needed.

3.4 General Discussion

While it is tempting to discuss each of the 71 objects discovered individually, I will not. Table 2 gives low-precision values of the orbital elements of all BSS discoveries, and Figures 16 and 17 show $a - i$ and $a - e$ plots for all objects detected in the BSS. Squares are objects that were known at the time of discovery, triangles are objects that were lost at the time of detection, and circles represent new discoveries. As these plots immedeately show, the BSS sampled all of the well-known high-inclination regions of the asteroid belt quite well, from the inner-belt Hungarias all the way to the Jupiter Trojans. Several totally new asteroid types were noticed, notably the new Hansa family (Hergenrother *et. al* 1996) and two tight congregations of objects just inside the 2:1 mean-motion resonance with Jupiter. Other unusual objects that do not fit into any classes are 1996 TT_5, 1977 TD, 1995 SX_{53} and 1995 SH_4. Several Mars-crossing types were discovered, including 1996 TY_9, the largest Mars-crosser to be discovered in the last 6 years, and a strong indication that the NEO population is only complete to absolute magnitude ~13.0. BSS is also responsible for some of the largest main-belt asteroid discoveries in recent times, with a handful of $H = 11$ objects. In addition, we discovered the closest approaching significantly sized NEO, 1996 JA_1, in May 1996 (see IAU Circular 6402, as well as "The Discovery and Physical Characteristics of 1996 JA_1, Spahr *et al* 1997). Several comets were detected, and a new comet, C/1996 R1 (Hergerother-Spahr) was discovered by us during September 1996 (IAU Circular 6470).

Table 1. Information on the BSS observing runs.

Dates	Fields	Area	Number Detections
March 15-17 1993	8	300	4
April 14-18 1993	13	450	5
May 14-18 1993	19	550	5
May 2-8 1994	20	600	7
June 2-12 1994	28	900	22
July 6-15 1994	41	1200	14
August 2-6 1994	24	700	5
December 28-31 1994	21	630	7
February 24-26 1995	23	630	11
May 20-31 1995	55	1650	20
June 24-26 1995	33	1000	23
August 26-Sept. 3 1995	40	1200	13
September 17-30 1995	41	1200	27
October 18-26 1995	41	1200	15
May 10-22 1996	60	1800	25
September 5-15 1996	43	1290	14
October 6-18 1996	53	1590	29
December 8-10 1996	16	480	11

Table 2. Orbital elements of BSS discoveries.

Object	a	e	i	H
1993 EL	2.70	0.3443	15.93	14.98
1993 GE	3.15	0.2334	25.82	11.30
1993 KQ2	2.35	0.2506	24.10	14.92
1993 HM1	2.65	0.1434	15.68	12.92
1994 JD	1.93	0.0775	23.54	14.55
1994 JS1	2.60	0.3514	19.45	14.08
6613	3.15	0.1804	25.45	11.90
1994 LL	2.70	0.0622	27.18	13.07
1994 LA1	3.15	0.2575	26.01	13.88
1994 NO	3.17	0.3321	20.69	14.05
1994 PK	1.94	0.0856	19.26	14.43
1994 PL	2.27	0.2356	23.34	13.80
1995 AN	1.97	0.0772	18.11	13.95
1994 YA2	2.65	0.0464	22.06	13.51
6534	3.17	0.1153	23.42	12.30
1995 DL1	3.16	0.2997	20.24	13.35
6533	2.64	0.0378	22.74	13.50
1995 DU1	2.32	0.1895	24.69	14.06
1995 KZ	2.35	0.1934	24.39	14.32
1995 KF	2.42	0.2803	22.77	14.83
1995 KO1	2.30	0.1928	24.55	15.11
1995 KA1	2.37	0.2316	19.85	14.73
1995 MX	2.80	0.2725	16.98	13.60
1995 QE2	3.05	0.2282	22.62	13.93
1995 QW3	2.31	0.1522	21.00	15.01
1995 QU3	3.15	0.3823	23.72	13.53
1995 RA	2.35	0.2322	22.99	13.50
1995 SA1	2.32	0.1577	22.63	13.94
1995 SO1	3.15	0.1536	21.25	13.82
1995 SR	2.59	0.3104	26.53	14.85
1995 SQ1	2.37	0.2226	23.72	14.80
1995 SB1	2.40	0.2536	24.33	14.92
1995 SS	1.82	0.0644	24.20	15.56
1995 SG4	2.29	0.2263	21.70	15.50

Table 2 (continued). Orbital elements of BSS discoveries.

1995 SC	2.76	0.3997	28.32	15.49
1995 SP1	3.13	0.2040	25.80	13.00
1995 SR1	3.15	0.0847	25.88	11.66
1995 SJ4	3.14	0.1352	20.23	13.50
1995 SB1	2.40	0.2536	24.33	14.92
1995 SB4	3.16	0.3887	22.96	15.00
1995 SX48	1.84	0.0224	21.99	15.00
1995 SW48	1.90	0.0850	24.82	15.50
1995 SW29	3.15	0.2025	25.53	12.60
1995 SX53	2.78	0.2534	22.57	14.50
1995 UR	2.30	0.2072	25.34	14.00
1995 UT6	3.07	0.3607	16.64	16.00
1995 US	2.99	0.1275	22.08	11.22
1996 JU	2.34	0.1811	24.76	14.00
1996 JV	2.41	0.1910	24.08	13.20
1996 JA1	2.56	0.6997	22.08	21.06
1996 KL1	3.10	0.2992	17.97	14.00
1996 RQ	1.92	0.0717	18.24	15.50
1996 RN2	1.93	0.0526	18.37	14.50
1996 RR2	1.91	0.0748	22.64	14.30
1996 RR5	3.15	0.3740	22.89	13.80
1996 RJ	5.20	0.0484	30.50	9.90
1996 TR5	2.36	0.2291	25.30	14.30
1996 TY8	2.42	0.2780	24.51	15.50
1996 TZ8	3.21	0.0596	20.61	12.80
1996 TW8	2.67	0.0677	21.32	12.80
1996 TX8	2.30	0.2450	24.27	14.90
1996 TS5	2.27	0.1892	23.62	13.60
1996 TT5	2.31	0.1897	18.15	15.00
1996 TY9	2.00	0.3158	29.73	13.00
1996 XU14	1.96	0.1104	16.33	15.06
1996 XQ18	2.72	0.2910	15.55	15.63
1996 XU14	1.96	0.1104	16.33	15.06
1996 XS23	2.29	0.2358	26.24	14.45

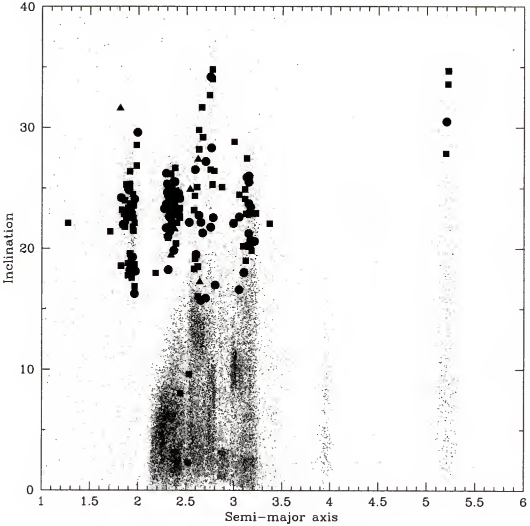

Figure 16. Semi-major axis and inclination for BSS detections. Circles represent new discoveries. Squares are objects known at the time of detection, triangles are those objects lost at the time of detection.

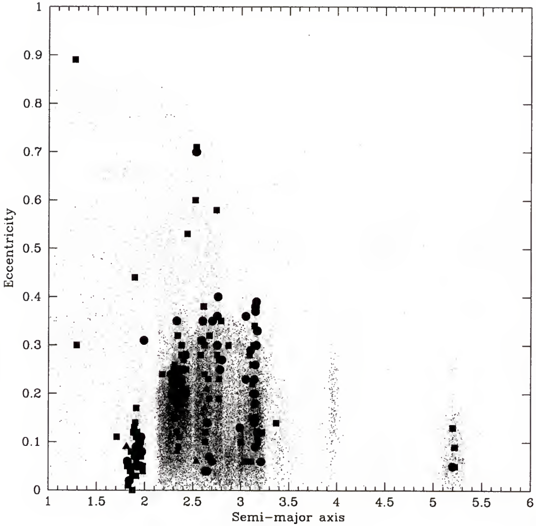

Figure 17. Semi-major axis and eccentricity for BSS detections. Circles represent new discoveries. Squares are objects known at the time of detection, triangles are those objects lost at the time of detection.

CHAPTER 4
DEBIASING THE PLS

4.1 How Does Debiasing Work?

The ultimate goal of this work is to remove the numerous observational selection effects present in a particular asteroid survey in order to present the best estimate of the true distribution of asteroid orbits and sizes. Without field centers, field sizes, observation dates, V magnitude and rate of motion efficiencies, debiasing is totally impossible. In addition we will need well-determined orbital elements for each object detected in a particular survey. For these reasons, all past surveys, save the PLS, MDS, and BSS are almost totally worthless for debiasing. This kind of detailed information for most asteroid surveys simply does not exist in the literature.

For the moment, I will assume that somehow I can calculate P, the probability of detecting a certain type of asteroid during a certain type of survey. This will certainly be a function of the asteroid's orbital elements a, e, and i, and probably H. For example, it would be impossible to detect an object at opposition with an aphelion distance less than the perihelion of the Earth's orbit (this places restrictions on the a and e combinations) or it would be impossible to detect an asteroid on a zero degree i orbit at the ecliptic pole. In these simple examples, we find that P is indeed a function of the orbital elements. One can also see that in general, P will be a very complicated function of orbital elements. If we also consider the V magnitude efficiency in the calculation of P, we find that simplistic interpretation of the bias becomes very difficult. P will be a function of how long the object is above the faint limit, and this will vary for different a and e combinations as well for different orbital orientations (in ω and Ω.)

If we had a table of P values for specific $a + da$, $e + de$, $i + di$, and $H + dH$ combinations for a particular survey strategy, and we had found some asteroids in our survey, N_f, with orbital element values in this range, the total number (N_T) in the asteroid belt for those element ranges would be:

$$N_T(a, e, i, H) = \frac{N_f(a, e, i, H)}{P(a, e, i, H)} \tag{4.1}$$

Summing this simple relationship over the entire range of orbital element space for the main belt will allow us to estimate the orbital element and absolute magnitude distribution of the asteroid belt from an asteroid survey, provided that P can be calculated.

4.2 How to Calculate P?

In their paper, Jedicke and Metcalfe (1998) present a general analytical technique for removing observational bias from asteroid surveys and apply this method to the Spacewatch survey (see Introduction and Chapter 2).

They assume that the angular orbital elements Ω and ω as well as M are distributed randomly, and that the system's V magnitude and rate of motion efficiency (ϵ) are known and compute ρ, the probability density of finding an asteroid with a, e, i at heliocentric distance r, latitude b, and longitude l to be:

$$\rho(a, e, i\,|r, \ell, b) = \frac{1}{2\pi^3}\frac{r}{a}\frac{1}{\sqrt{2ar - r^2 + a^2(e^2 - 1)}}\frac{\cos b}{\sqrt{\sin^2 i - \sin^2 b}} \tag{4.2}$$

To determine the probability of detecting an asteroid at a geocentric right ascension (RA) and declination (DEC), this heliocentric probability density must be converted to a geocentric probability density by means of the Jacobian, and then must be integrated over the limits in RA and DEC of all of the fields, j, and over the geocentric distance, Δ:

$$\begin{aligned} P(a,e,i) &= \sum_j \int_0^\infty d\Delta \int_{\alpha_j^{min}}^{\alpha_j^{max}} d\alpha \int_{\delta_j^{min}}^{\delta_j^{max}} d\delta \\ &\times \; \rho(a,e,i;r,\ell,b) \left| \frac{\partial(r,\ell,b)}{\partial(\Delta,\lambda',\beta)} \right| \left| \frac{\partial(\lambda',\beta)}{\partial(\alpha,\delta)} \right| \epsilon(a,e,i;r,\ell,b;\Delta,\lambda',\beta,...) \end{aligned}$$

While we know that Ω and ω are not randomly distributed, Jedicke and Metcalfe had no way of dealing with this because their data set contained objects with forced-fit circular orbits, and allowed no determination of Ω and ω (see Section 2.6). As will be discussed later, assuming randomly distributed elements only slightly affects P.

Since Jedicke and Metcalfe made the first real attempt at determining P for an asteroid survey, they had no way of determining if their method was correct. After several discussions with Jedicke in October 1996, I decided to develop my own method for determining P, this time using a purely numerical technique. This would allow a rigorous independent check of Jedicke's work, as well as have more versatility than his method.

4.3 The TBS Monte-Carlo Method for Detection Probabilities

This Monte-Carlo technique, dubbed the TBS method (from my initials) for calculating P is quite simplistic, yet it reproduces the results of Jedicke and Metcalfe quite well, and does in fact have some advantages over their method. The TBS method generates a synthetic population of asteroids, with a full set of orbital elements suitable for predicting the location of each object, using a set of calls to a random number generator. This file of orbital elements is input to a program, 'simulate', that contains a simple 'search' type algorithm that determines whether or not a particular asteroid is detected in a particular field at a specified time. If an object is detected, it is put in a file that contains the orbital elements, the V magnitude, H value, and any other desired information. These detections are parceled into small bins of a, e, i, and H, and the number in each bin, $N_d(a,e,i,H)$ is counted. To mimic a particular survey, I include $\epsilon(V, r)$, the system's V magnitude and rate of motion, r, efficiencies. To determine P, all that has to be done is to find $N_g(a, e, i, H)$, the number generated in the same bins, and compute the following fraction:

$$P(a, e, i, H) = \frac{N_d(a, e, i, H)\epsilon(V, r)}{N_g(a, e, i, H)} \tag{4.3}$$

P is defined as the *instantaneous* probability of detecting an asteroid of type $a + da, e + de, i + di, H + dH$ in a field at the specified RA and DEC. For a set of fields, individual P values can be summed to get P for an entire survey, or a particular survey strategy. Note that if ϵ is not considered, we are only asking how often a particular type of asteroid appears in a specific field, and not whether or not it is detectable, and in this case the detection probability is independent of H. This should be obvious, since H contains no information on the position of the asteroid.

For direct comparison with the Jedicke and Metcalfe method, I ran both my combination of programs and the Jedicke and Metcalfe code on the same field centered on the ecliptic, 9.9 × 9.9 degrees square, at opposition. Because Jedicke and Metcalfe assume that M, Ω, and ω are random and uncorrelated, my first simulation followed this assumption. The results of this test indicated that the methods produced nearly identical results, so I ran another simulation using the orbital element distribution of the observationally complete set of asteroids as defined in Chapter 1. A total of 261 bins of a,e and i space from a = 2-3.5, e = 0.005-0.355 and i = 0.5-20.5 were compared. Note that it is impossible, using the Jedicke and Metcalfe method, to find P for an object on a zero degree inclination orbit, or an orbit with zero eccentricity because an infinity will be produced in the ecliptic (see equation 4.2), and thus I had to restrict the i range to greater than 0.5 degrees and e to greater than 0.005. Figure 18 shows a histogram quantity P(TBS)-P(JM) / P(JM). Note that the mean value of the percentage difference is around zero, and that the maximum error is only 48 %. Individual comparison with the orbital elements (Figures 19-21) shows that the

Jedicke and Metcalfe method has no systematic effects, save a slight trend in the eccentricities. It is thought at this time that this trend is due to the fact that Jedicke and Metcalfe assume that the Jacobian in equation 4.3 is constant thoughout the acceptable range of geocentric distances for the main belt, an assumption that will not be precisely correct for objects with small geocentric distances, as some high-e objects will have. To ensure that I am comparing methods fairly, I only compared those bins in which I had a large number of detections and generated objects. Because the error goes as $\sqrt{N_d}$, this ensures that the error in the TBS method will be minimal. A larger simulation on a field around the Vernal Equinox (Jedicke and Metcalfe 1998) also shows the methods agree, and that the errors are smaller. The non-dependence on the main orbital elements is to be expected from both methods, in the sense that P is independent of the distribution of a, e, and i in both methods. Notice that in equations 4.1 - 4.3 there is no dependence on the distribution of of these elements themselves. While future tests will be run to explicitly determine the dependence on the angular elements, this is a bit beyond what will be undertaken on here. The main point here is that the methods are nearly identical, and the most time-efficienct method should be chosen for a particular survey stragey. At present the preferred method is the Monte-Carlo method, and this is discussed in Section 7.1 of this Thesis.

4.4 How Does P Vary for a Standard Field?

For a standard field, 1 degree by 1 degree at the Vernal Equinox at opposition, Figure 22-23), with a V magnitude faint limit = 20.0, one can see how P varies as a function of the orbital element combinations. In the first panel, P, (called by Jedicke and Metcalfe the bias), is plotted for i = 2.75 degrees and H = 8.0, panel 2: H = 10.5, panel 3: H = 13, and panel 4: H = 15.5. For the largest and brightest objects, P is highest for large a and e. This is intuitive: these objects move the slowest and thus spend more time than other objects in the fields in question. Note also that as H changes, P *does not* vary until H becomes large enough to push the object below the faint limit for some fraction of the object's orbit (last panel). Note that for the brightest objects, as a increases, so does P, and as i increases (the second set of figures) from 2.75, 12.75, 22.75 and 32.5, P drops dramatically. The complicated a and e dependence on P shown in the 4th panel of Figure 22 is just the type of behavior that will not be properly handled by a piecewise solution to debiasing based on general correction factors and mean magnitudes, and illustrates the need for a general technique for calculating P using the orbital elements and absolute magnitudes.

4.5 Application to the PLS

At this point I was convinced that the JM method was calculating the proper detection probabilities, and it would be simple to apply their method to the PLS. It was necessary to modify their code to deal with rectangular fields instead of Spacewatch scans. I obtained the complete set of PLS orbital elements from Gareth Williams and Brian Marsden at the SAO/IAU/MPC in order to bin their data in small bins of a,e,i and H for division by the appropriate detection probability, and to determine the PLS V efficiency.

4.6 Determination of the PLS V Magnitude Efficiency

While the authors of the PLS claimed a nearly 100 % magnitude efficiency in all but the last magnitude bin (V = 19.5-20), I chose to compute this quantity from their data independently.

The PLS authors reported positions of all objects detected to the Minor Planet Center. Note that the distinction between a discovered object and an object already known is not important for debiasing. A total of 1232 objects were detected in both months, 901 only in September and 236 only in October. The nearly 700 object difference is in the fact that the October fields were shot as to maximize the number of September objects recovered. The 236 objects detected only in October drifted into the October fields from above or below the September fields, and 331 objects found in September only had motions that took them out of the range covered by the October plates.

To determine the V efficiency, I ran my 'simulate' program on the PLS October fields with the file I obtained from the MPC and kept track of the objects that were actually in the fields but not detected, as well as those objects that were detected. A total of 1466 objects were detected on October plates and if I can assume that the 716 objects not found on the October plates, but that should have been found (i.e., they were within the RA and DEC limits of the fields but were missed due to their faintness and not for any other reason such as rate efficiency or error in the orbit computation), I could then compute the V magnitude efficiency by simply dividing the number of objects detected as a function of V by the number of objects detected + missed. The detection efficiency is presented in Figure 24, and it is quite close to what the authors actually quoted. This is also a testament to what can be done with properly obtained photographic data. A detection efficiency of over 90% at the $V =$ 19 level has not yet been achieved by any CCD asteroid survey program.

4.7 Why the PLS Will Underestimate the True Numbers of Asteroids in Each *H* Bin.

Of some worry in this calculation is the fact that we are only considering the objects that had orbits calculated. Some small fraction of PLS objects, the fraction unknown at this stage, were observed on only one or two nights. This will change both the V efficiency and P, but we have no way of determining the effect at this time. In addition and perhaps more important is the fact that we do not know how many PLS objects were detected on multiple nights due to overlap between the fields. These multiple detections must be included in the set of orbits we use for debiasing because the calculation of P takes into account the overlap between the fields. Because of these two effects the debiased PLS results will be noted as strict lower limits to the actual set of asteroids in the main belt.

4.8 The Trend with Longitude of Perihelion

As noted earlier, there is a definite trend in the number of objects as a function of longitude of perihelion (see Figure 2). While this cannot be taken into account with the Jedicke and Metcalfe method, the TBS method is very well suited to deal with this type of trend. As evidenced by various simulations described earlier, however, this trend has a relatively small effect on the actual bias values and for all practical purposes can be ignored. It is most likely because the observed distribution of M and ϖ is always quite close to the actual distribution of these elements, regardless of what time of year the survey is being conducted. In a sense, the bias-free set of M and ϖ can easily be observed, and this is very insensitive to survey strategy. Several simulations of PLS-type surveys conducted at different times of the year confirmed this: the observed ϖ distributions were always very similar to the actual distribution. The accompanying trend in mean e can largely be ignored, because it results in only a ~ 0.5 magnitude difference for an average asteroid, and this is about the practical limit of determined V magnitudes, and hence H values.

4.9 Results

The debiased a, e, and i distributions are presented in Figures 25-27. The bin sizes are 0.05 AU, 0.05, and 5 degrees respectively. These distributions are including data from all three zones. Note that I am only using objects from H = 13-15.5. I have chosen to plot this size range, and to normalize each plot to the total number in this H range (71575) in an effort to compare these regions of the belt fairly. Simply plotting total numbers in each bin would have led to a bias toward the inner belt, since there P was computed for objects with $H = 16.5$, while the middle belt and outer belt were only debiased to $H = 15.75$ and 15.25, respectively. Also included in each figure is the distribution of the observationally complete set as defined by Jedicke and Metcalfe (1998).

The semi-major axis distribution Figure 25 shows the a distribution. This can be compared with that for the observationally complete set (Figure 10), and some dramatic differences are evident. While the peaks in both diagrams match, in general, in the inner belt, the outer belt shows some striking differences. In the debiased Figure, the 5:2 mean-motion resonance appears much deeper than that of the observationally complete set. The most populated bin in the debiased set at 3.075 AU is one of the least populated bins in the observationally complete set. While there is not enough information to do other than speculate, it would seem that there must be additional members of the Eos and Themis families that 'leak' or diffuse into these neighboring bins. The largest peaks in the debiased plot are from the main asteroid families Maria at $\sim$ 2.6 AU, Koronis at $\sim$ 2.8 AU, Eos, which is split between two bins at $\sim$ 3.0 AU, and Themis at $\sim$ 3.18 AU. Some error is to be expected because of placement of the bins, although I used the same bin sizes an limits for each graph.

The eccentricity and inclination distribution Figures 26 and 27 show the e and i distributions. These are remarkably close to the distribution of these elements for the observationally complete set.

The slope of the size-frequency distribution Figures 28-31 show the the distribution of H in half-magnitude bins for each of the three zones, and the sum of the three zones. It seems very likely that α is quite close to 0.45 for the whole of the main belt, and this translates to a mass index, q, of 1.75, as compared to the Dohnyani value of 1.833. With our error bars, this is completely consistent with the work of Durda (1993), and most likely excludes Dohnyani's value. Table 3 lists the α and q values for the debiased PLS. Note that α has been computed from the $H = 13.25$ bin to the extent of the debiasing in H. This should allow fair comparison between regions of the belt. A change in the range of H fit the least-squares solution will change the α value. Starting at H of 13.25 is probably best because we expect α to be linear beyond this point. However, using the debiased Spacewatch data from Jedicke and

Metcalfe (1998), Durda *et al.* (1998) have found a deviation from non-linearity in the H distribution. While this may be true, our data are not of sufficient precision to detect this. Because of the problems already mentioned with Spacewatch debiasing, the Durda *et al.* result must be viewed with some skepticism. Future surveying and debiasing will be the only way to resolve this issue.

In this entire section, error bars were computed using Poisson statistics. For instance, if there were 100 objects detected in a particular bin of a, e, i, and H, then the error would be $\sqrt{100}/100$, or 10%. While the number of detections is usually quite small, the error bars are nonetheless very small becase the errors get added in quadrature.

4.10 Additional

It will be noted here that the direct conversion of α to q is fraught with uncertainty. Asteroid H values are dependent on the albedo based on the following equation:

$$2log(D) = 6.241 - 0.4H - log(p_v) \tag{4.4}$$

with p_v being the albedo in the V passband. The spread p_v is quite large in the asteroid belt, ranging from around 0.02 to 0.40. Mean values in the three zones have been determined from the IRAS data (which I pulled directly from the PDS Small Bodies Node web site, URL:

http://pdssbn.astro.umd.edu/SBNast/holdings/IRAS-A-FPA-3-RDR-IMPS-V3.0.html

and are listed in Table 4. There is certainly some uncertainty in this data set, as IRAS could only observe the largest objects. Precise albedoes for most of the numbered asteroids is essential for future studies of the size distribution.

Table 3. α and q values determined from the debiased PLS.

a range	α	q
2-2.6 AU	0.4528 ± 0.0312	1.755 ± 0.052
2.6-3.0 AU	0.4816 ± 0.0264	1.802 ± 0.044
3-3.5 AU	0.489 ± 0.0912	1.815 ± 0.152
2-3.5 AU	0.4582 ± 0.0474	1.763 ± 0.079

Table 4. p_v values as determined from the IRAS database.

a range	p_v	number of objects
hline 1.8-2.0 AU	0.2256 ± 0.025	7
2-2.6 AU	0.1501 ± 0.006	301
2.6-3.0 AU	0.1244 ± 0.004	588
3-3.5 AU	0.0941 ± 0.002	912

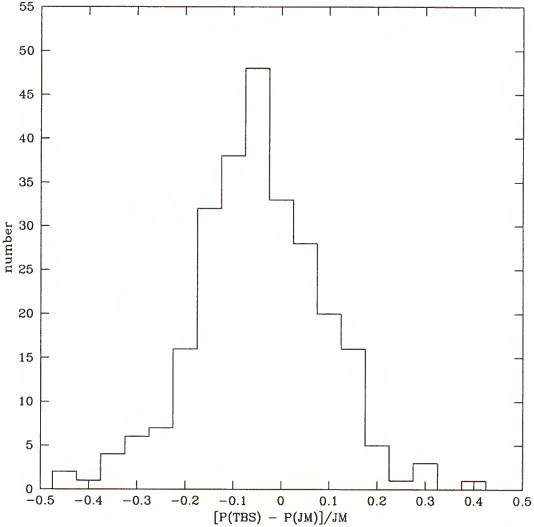

Figure 18. Comparison of the Spahr method to the Jedicke and Metcalfe method for computing detection probabilities.

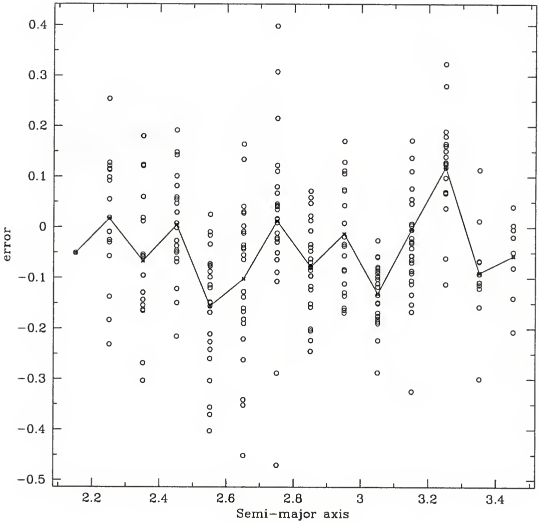

Figure 19. Comparison of the Spahr and Jedicke and Metcalfe methods for debiasing in semi-major axis.

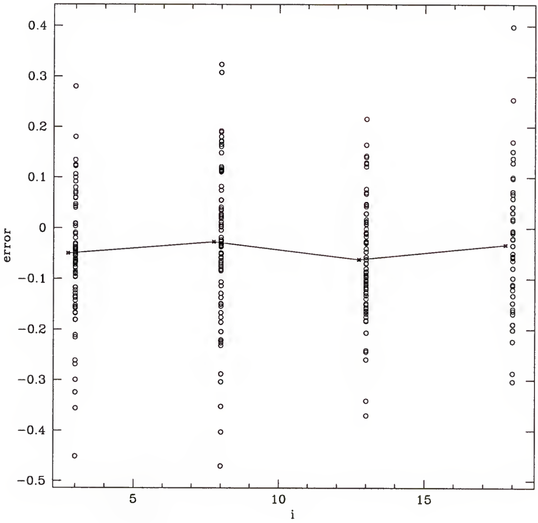

Figure 20. Comparison of the Spahr and Jedicke and Metcalfe methods for debiasing in inclination.

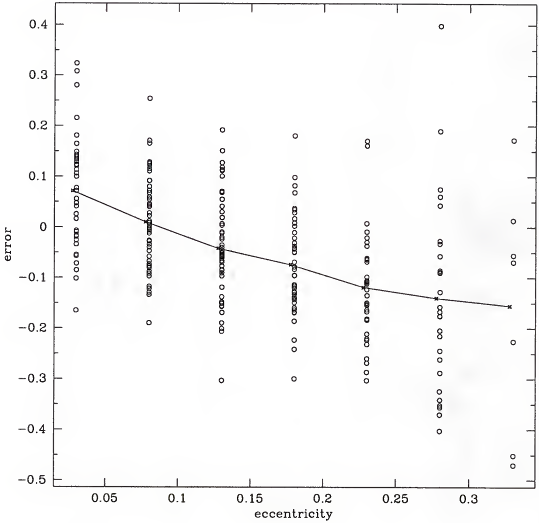

Figure 21. Comparison of the Spahr and Jedicke and Metcalfe methods for debiasing in eccentricity.

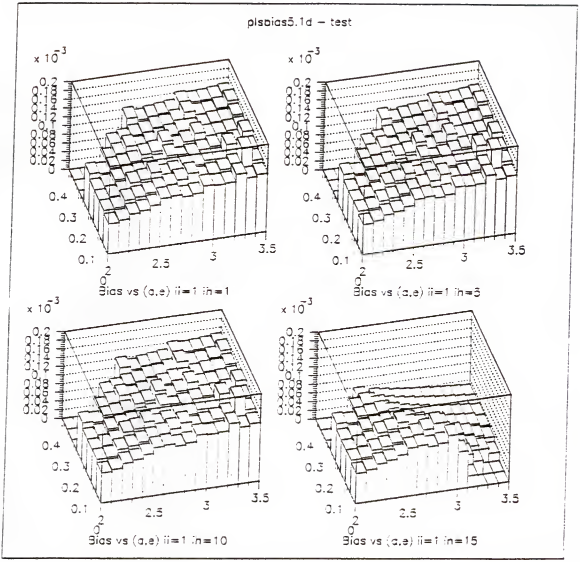

Figure 22. Detection probabilities for a standard field as described in the text.

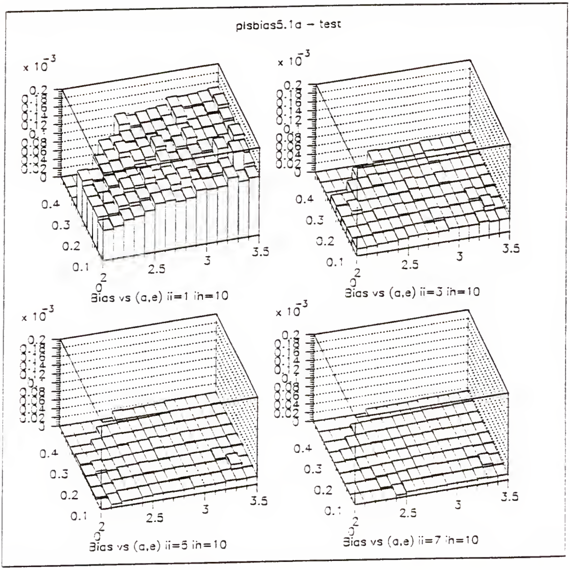

Figure 23. Detection probabilities for a standard field as described in the text.

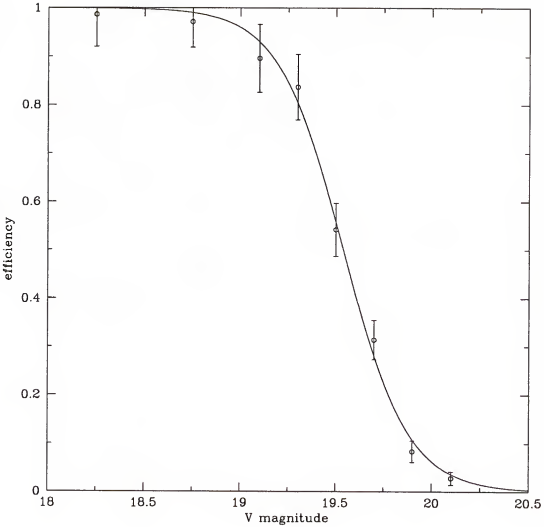

Figure 24. PLS *V* efficiency as determined in the text.

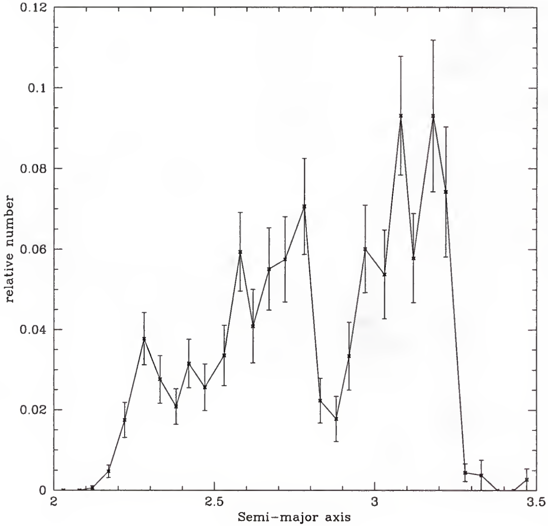

Figure 25. PLS debiased semi-major axis distribution for objects with H between 13 and 15.5

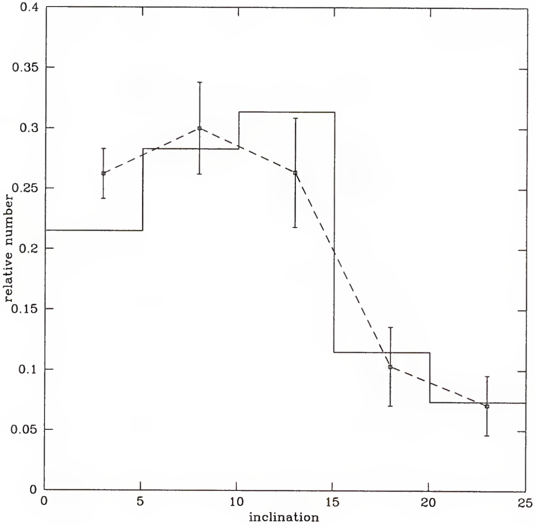

Figure 26. PLS debiased inclination distribution for objects with H between 13 and 15.5. Also included (histogram) is the observationally complete set.

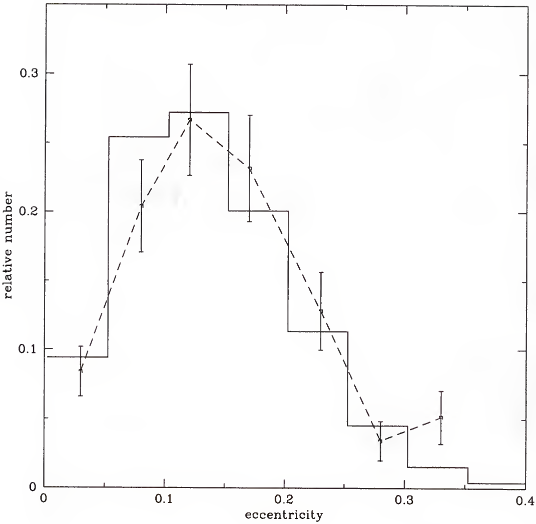

Figure 27. PLS debiased eccentricity distribution for objects with H between 13 and 15.5. Also included (histogram) is the observationally complete set.

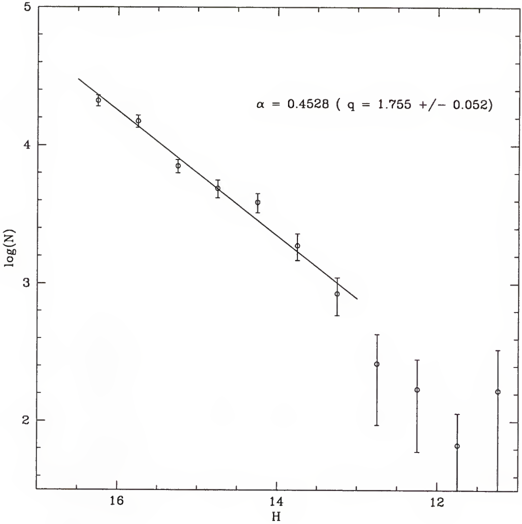

Figure 28. α value for semi-major axis range 2-2.6 AU.

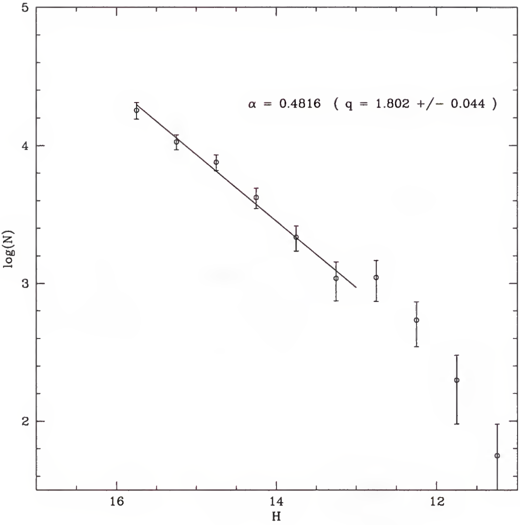

Figure 29. α value for semi-major axis range 2.6-3 AU.

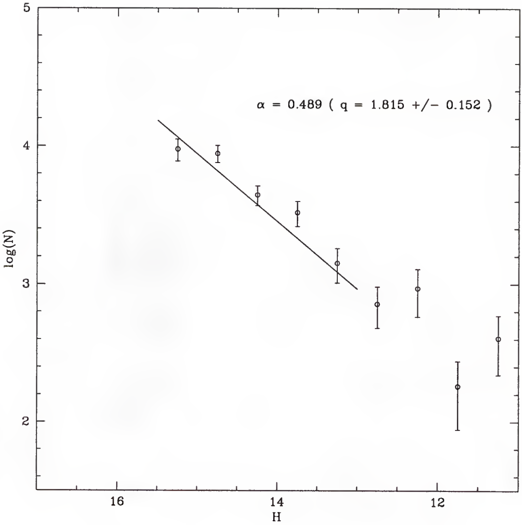

Figure 30. α value for semi-major axis range 3-3.5 AU.

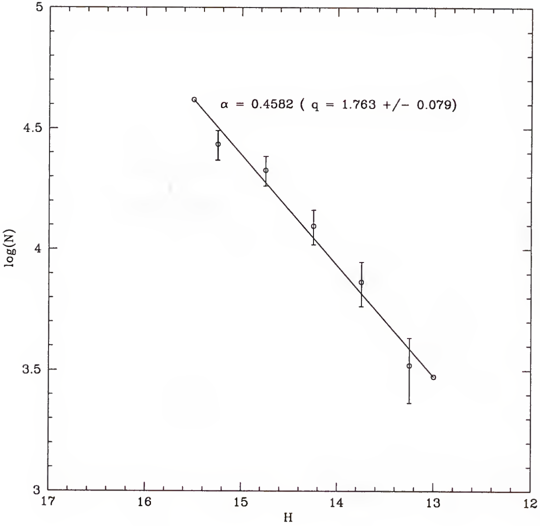

Figure 31. α value for semi-major axis range 2-3.5 AU.

CHAPTER 5
DEBIASING THE BSS

5.1 Introduction

The Jedicke and Metcalfe method works well for populations of asteroids that have nearly random orbital elements. But this is not the case for high-inclination objects. Figure 32 shows a plot of Ω and i for the Hungaria population, and indicates that these elements are strongly coupled. BSS was conducted at high ecliptic latitudes, and because slight displacement from the ecliptic will produce a strong bias in Ω (Bowell *et al.* 1989), this also produces a bias in i. In other words, during different times of the year, BSS will sample different areas of the inclination distribution for Hungarias. Or perhaps it is clearer to say that the probability of detecting a Hungaria with a specific inclination is not constant throughout the year, as is explicitly assumed in the Jedicke and Metcalfe method. Because of the strong effect i has on the bias for ecliptic surveys, this type of element coupling must also taken into account by those wishing to use ecliptic survey material for debiasing the high-inclination asteroid populations.

To escape this element coupling problem, I used the TBS method described in the previous chapter for detection probabilities, but I chose an input orbital element distribution that closely matched those high-i objects I wished to debias. This was accomplished by looking at plots of the orbital elements for only the brightest members (ie, those objects at which we expect observational completeness) for the Hungaria and Phocaea populations, and generating simulated populations of asteroids that closely matched the actual distribution. Since the Hungaria and Phocaea populations occupy small regions of orbital element space, the exact orbital element distribution is probably not critical in a, e and i (see also the previous Chapter), but the distribution of angular elements and correlations with e and i and the angular elements must be taken into account. For the region 2.6-3.3 AU, I used the TBS method but assumed that the orbital elements were randomly distributed. At present, objects are simply too sparsely distributed, and the range of orbital element space is too large, to justify using any assumed orbital element distribution other than random.

5.2 Generated Objects and Detection Efficiency

As mentioned in the previous chapter, P is independent of H if the magnitude efficiency is not considered. With this in mind, I generated large populations of Hungarias and Phocaeas (100,000-500,000 objects) following the assumed orbital element distributions, but assuming that $H = 0$, and ran these through my simulation program on the BSS fields. The output file has a column for H, and the V(H=0) magnitude. Since the V and H relationship is linear, I could open my output file, loop over the H ranges I was interested in, and calculate new V magnitudes from the simple relationship $V(H) = V(0) + H$. In this step, I included the magnitude efficiency. A simple call to a random number generator for each detected object checked to see if the object was within the detectable range of magnitudes, and if the object would actually be detected based upon the efficiency. This elegant approach allows many more objects to be generated, reducing the error in the determination of P, as the dominant term in the error is in N_d, the number detected. This has the effect of N_g objects in *each* H bin. Note that the magnitude efficiency can be considered in the final step, and that the TBS method does not require new simulations with different magnitude efficiencies as does the Jedicke and Metcalfe method. Rather than try to calculate the V detection efficiency as was done in the previous chapter, I simply assumed a high, best estimate, and low detection efficiency. Note that the best estimate is not the average of the low and high efficiencies. The best estimate is based on some observer tests using opposition fields with many asteroid detections, and, for lack of any other input, gut instinct. Figure 33 shows the different efficiencies. It should be noted that the efficiency is notoriously difficult to compute for a photographic survey with few detections, and one conducted over several years. Many factors, such as the observer's mental state, how well rested he was, how well the films were developed, as well as weather conditions can all affect this quantity. As will be seen later, these varying efficiencies do not affect the BSS as much as one would suppose, and also has the benefit of allowing systematic error studies.

Because the total number of BSS detections is small, I used the maximum likelihood method for determining the slope, α, of the absolute magnitude distribution. This method is best for small-number data sets, as it is ideal for minimizing errors in the fact that it requires no binning of the data. Jedicke and Herron (1997) used this method with success on the Centaur population based on Spacewatch data. This method requires an assumption about the parameter that we wish to determine; in this case we assume that the absolute magnitude-frequency distribution is linear. First we find l, the likelihood, from:

$$l = \frac{\sum_{d=1}^{N_d} 10^{\alpha H_d} \epsilon(H_d)}{\int 10^{\alpha H} \epsilon(H) dH} \tag{5.1}$$

where ϵ is the survey's detection efficiency as a function of H, N_d is the number of detections, H_d is the value of H for a specific detection, and the integral in the denominator is over the entire range of H sampled. $\epsilon(H)$ is found from taking the standard detection probabilities computed as a function of the elements a, e, i, and H, and reducing them to P(H), the marginal distribution. Once $\epsilon(H)$ is determined, we simply find where log(l) is a maximum by varying α and re-computing l by means of a simple computer program. This method also gives estimates for the statistical error by simply finding where the log(l) value has dropped by 0.5. Systematic error studies will be discussed below. For determining the orbital element distribution, standard debiasing techniques as described in Chapter 4 are used, provided that we limit our range of H such that we do not have very small detection probabilities for the denominator of equation 4.1.

5.3 Results

For the Phocaea and Hungaria populations, I was able to determine the α, as well as the a, e, and i distributions. Use of the maximum likelihood method prevents determination of the orbital element distribution, but this can be determined from standard debiasing techniques, provided that the absolute magnitude space is restricted to the brighter ranges, or those where the detection probability is not too small. While this is one disadvantage to the maximum likelihood method, an advantage is that we place very solid constraints on α. Since I used different V efficiencies, I could place upper and lower limits, which amount to *systematic* error bars, on α. For the Hungaria population, I find $\alpha = 0.5 \pm 0.2$, while the Phocaea population has $\alpha = 0.46 \pm 0.12$. Figures 34-35 show the H efficiency, and a plot of log(l) from one of the runs for Phocaeas, with the maximum α value noted as well as the 1-σ error values.

Because of the large volume of phase space in the main belt range (a = 2.6-3.3 AU, i = 15-35 degrees, e = 0-0.4), the detected numbers are significantly small that I did not attempt to determine α, although some general trends in orbital elements can be determined.

5.4 General Trends in the Region a = 2.6 - 3.3 AU

The inclination limit. While this region is home to some very high i objects, it appears that they are still very uncommon. BSS only detected 5 objects with $i >$ 30 degrees, and one of these was (2) Pallas. Over the entire BSS, P is very high for the bright, large i objects, and BSS can place very strong constraints on these. The only 40 + inclination main belt detection is (2938) Hopi, and thus we must conclude that objects with inclinations over 30 degrees are very rare. Rough debiasing gives 50% of the objects in the i range 15 to 35 degrees in a 5-degree bin centered at $i = 17.5$, with 37% in the next bin at 22.5 degrees, 9% at 27.5, and 2% at 32.5.

The eccentricity distribution. One general trend that is easy to notice in this range of a and i is the high mean eccentricities. Within the error bars, the e distribution from 0 to 0.40 is totally flat. This is drastically different than that of the lower inclination regions, with the mean e being around 0.13, and showing a Poisson-type distribution. The Pallas region is known to have many large-e objects, and as will be mentioned below, an apparently large new congregation of objects near the 2:1 resonance with Jupiter is also contributing. There is a strong dynamical reason for this type of trend, namely that the important terms in the disturbing function tend to have products of e and i, indicating that these elements are strongly coupled.

The semi-major axis distribution. The a distribution is quite different than that for the lower i ranges covered by the PLS and Spacewatch, but this is expected because of the lack of large families at higher i. Roughly 63% of the objects are in the range a = 2.5-2.68 AU, 10% in the range 2.68-2.85 AU, 4% in the range 2.85-3.03 AU, and 22% 3.11-3.29 AU. The inner two bins presumably are affected by the 5:2 resonance, which appears to be nearly devoid of high i objects. The new Hansa family (see below), as well as the Maria family are contributing heavily to the first a bin. Figure 36 shows the a distribution for objects with i greater than 15 degrees, from the Hungaria population to the 2:1 mean-motion resonance with Jupiter.

5.5 New Families

Hergenrother *et al.* (1996) presented the discovery of a new asteroid family associated with (480) Hansa ($a, e, i = 2.64, 0.05, 21.3$) based on 3 new BSS discoveries, namely (6533), 1994 YA_2 and 1996 TW_8. The detection probability for these objects is quite small, as they only just enter the lower fields of the BSS survey area. A rough estimate is 150 ± 100 objects down to $H = 13.5$, indicating this to be a fairly sizeable family, and in fact comparable in number to the entire Hungaria group.

In addition to the Hansa family, there may be more asteroid families in the data. Two groupings near the 2:1 resonance with Jupiter could possibly be families, but proper elements are notoriously difficult to calculate and interpret for objects in this area. We will list these objects here in hopes that future work will answer this question. The first suspected family is associated with (31) Euphrosyne (3.15, 0.23, 26.3) , and consists of (6613), (7476), (7605), 1994 LA_1, 1995 SP_1, and 1995 SW_{29}, while the second suspected family appears to have no known primary member, and is associated with (7200), 1995 DL_1, 1995 QU_3, 1995 SB_4 and 1996 RR_5 (mean elements around 3.16, 0.35, 23). We suspect that these are new families or groupings similar to the Phocaea and Hungaria populations because the projected number in bins of (a,e,i,H) centered on the mean value for each much higher than for neighboring bins. The estimated total number of members in Group 1 is 35 ± 10 to $H = 14$, while Group 2 is more populous, with 110 ± 50 to $H = 15$. Group 2 is interesting in that the objects have large aphelion distances (> 4.2 AU), but appear to be protected from close encounters with Jupiter by virtue of their large inclination and ω values of either 90 or 270 degrees placing them several AU below the ecliptic at aphelion. Long-term orbital integrations (Scotti and Spahr unpublished) have shown the objects to be stable over at least 10^7 year timescales, and shows enormous variations of 15 to 45 deg in i and 0 to 0.5 in e respectively.

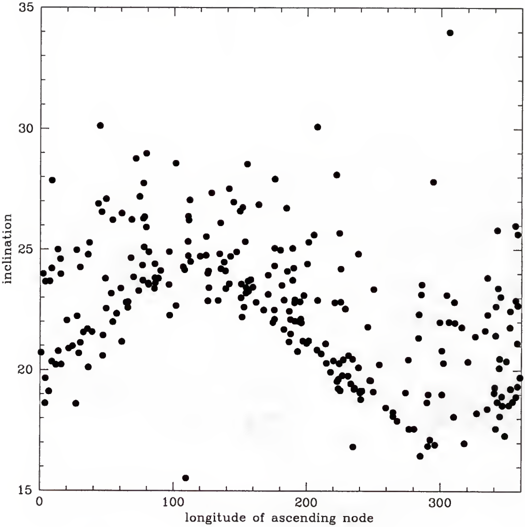

Figure 32. Trend in inclination and longitude of ascending node for known Hungarias.

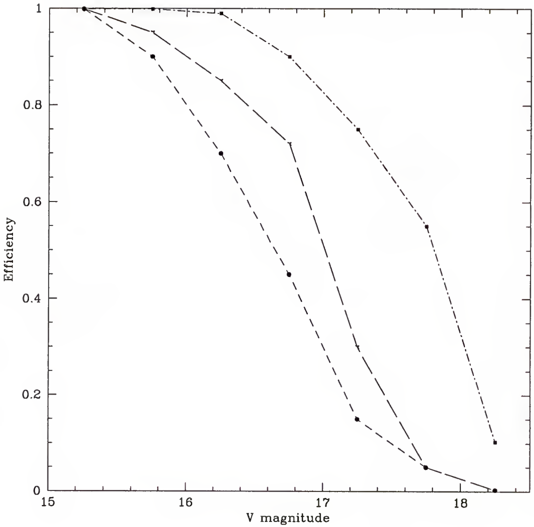

Figure 33. BSS V magnitude efficiency parameters.

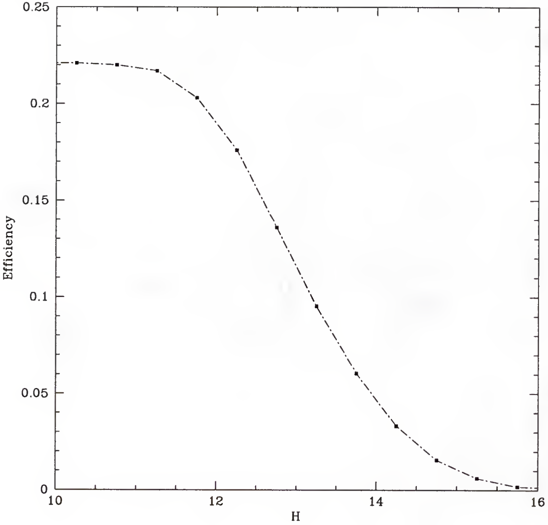

Figure 34. Marginal distribution in H for Phocaeas detected in the BSS using the middle V magnitude efficiency.

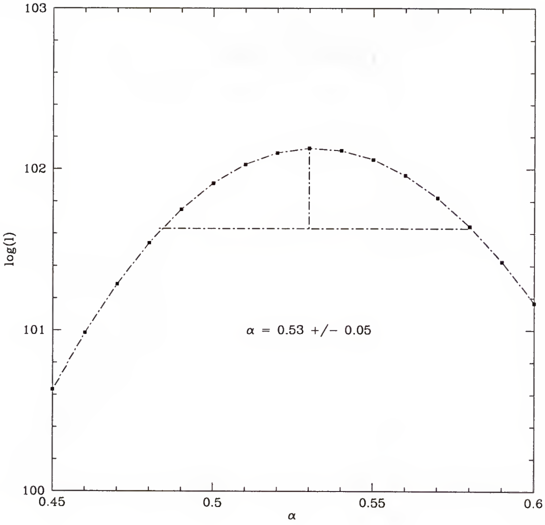

Figure 35. Maximum likelihood method applied to Phocaeas detected in the BSS using the middle V magnitude efficiency.

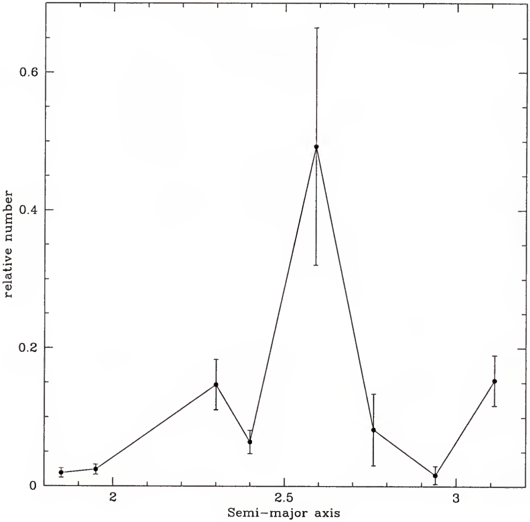

Figure 36. Semi-major axis distribution for objects with inclinations greater than 15 degrees based on BSS predicitons.

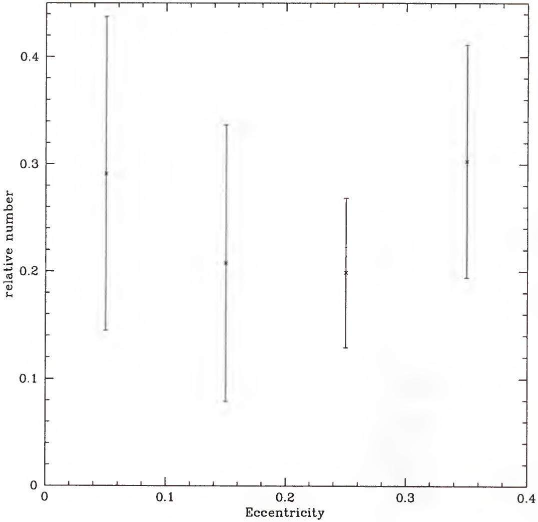

Figure 37. Eccentricity distribution for for objects with inclinations greater than 15 degrees based on BSS predictions.

CHAPTER 6
WHERE IS THE BEST PLACE TO LOOK FOR CERTAIN TYPES OF ASTEROIDS?

6.1 The General Concept

The concept of asteroid detection probabilities lends itself to many other uses than simple debiasing. For instance, this technique would allow an observer to find the most likely location of the sky to detect certain types of asteroids. As telescope time is scarce, and even more so for asteroid survey teams, efficiency of survey strategy must be considered.

It is a commonly held belief that surveying on the ecliptic will produce the most asteroid discoveries. It turns out that this will be true for only the lowest inclination asteroids. In the simple case of a circular inclined orbit, the Z equation as a function of time will be identical to the simple pendulum equation in one dimension. Since the pendulum spends most of its time at the top of the swing, where the velocity is slowest, higher inclination asteroids will spend most of their time at higher ecliptic latitudes, rather than in the ecliptic.

6.2 Quantitative Study: Eos and Maria Family Asteroids

The size distribution of asteroid families is fundamental to our understanding of collisional processes. Due to observational incompleteness, we have little information beyond $H = 11$ for the major asteroid families, and this makes determining anything useful regarding the collisional history difficult. The Eos family at $a = 3.01$, $i \sim 10$ will be strongly effected by observational incompleteness due to the large a value, and the moderate i. One way to improve this situation would be to conduct a *directed* survey, aimed specifically at the best location in the sky to find Eos family asteroids. In order to determine this best location, I created a population of 150,000 synthetic Eos family members and ran this through my simulation program at opposition longitudes, λ, 0 to 120 degrees and β 0 to 20 degrees. At opposition, where the objects are brightest, 75 % more Eos family members will be found at 10 degrees β than at 0 degrees β. Moving away from opposition greatly increases the detected number, rising to 300 % of the opposition value at 7 degrees β and 120 degrees λ. One must contend with the fact that objects at 120 degrees from opposition will be $\sim$ 2 magnitudes fainter than at opposition, and that there will be considerably less time for observation in this area of the sky. But the simple fact that in the ecliptic opposition is *not* the best place in the sky to look for Eos family asteroid cannot be avoided. Table 5 lists the ratio of the number of detected Eos family members to the number of these objects detected at 0 degrees λ and 0 degrees β as a function of λ and β. Table 6 shows the same for a similar simulation of Maria family $a = 2.6$ AU, $i = 15$ degrees.

This type of behavior is expected from the nature of asteroidal orbits, and simple geometry. The equation

$$\sin(\beta) = \frac{r}{\Delta}\sin(i)\sin(\omega + f) \tag{6.1}$$

defines the geocentric ecliptic latitude as a function of the inclination, i, the heliocentric distance, r, the geocentric distance, Δ, the true anomaly, f, and the argument of perihelion, ω. Since r/Δ is around 2 for most main belt objects at the maximum, the maximum ecliptic latitude attainable will be $\sim 2 \times i$. Objects will also linger around this value of β longer than other β values because the asteroid will be reversing its direction at the top, ie, the Z velocity must drop to zero, and change sign. As we move away from opposition (resulting in an increase in Δ), r/Δ will be near to or slightly less than unity, and this explains the high concetrations of Maria and Eos family asteroids at β values near or slightly less than their i value as we move away from opposition.

Table 5. Longitudes from opposition (λ), ecliptic latitudes (β), and the ratio (ρ), of objects detected at (λ, β) to that detected at (0,0) for Eos family asteroids.

λ	β	ρ	....	λ	β	ρ
0	+10	1.65	....	30	0	1.08
0	+15	1.52	....	30	+10	1.48
0	+20	0.44	....	30	+15	1.51
60	0	1.54	....	90	0	1.95
60	+10	2.40	....	90	+7	3.13
60	+12	1.87	....	90	+10	2.56
120	0	2.83	....			
120	+5	4.06	....			
120	+7	3.30	....			

Table 6. Longitudes from opposition (λ), ecliptic latitudes (β), and the ratio of objects detected at (λ, β) to that detected at (0,0) for Maria family asteroids.

λ	β	ρ	....	λ	β	ρ
0	+10	1.21	....	30	+10	1.25
0	+15	1.54	....	30	+15	1.65
0	+20	1.98	....	30	+20	2.13
60	0	1.77	....	90	+10	3.89
60	+15	2.87	....	90	+13	4.38
60	+20	2.24	....	90	+15	3.66
120	+5	5.21	....			
120	+10	4.70	....			

CHAPTER 7
SUMMARY

7.1 Conclusions

The main conclusions of this work are as follows:

1) We have created a new technique to remove observational selection effects from asteroid surveys. This has verified the conclusions of Jedicke and Metcalf (1998). Our method is more versatile than the Jedicke and Metcalfe method, and is unaffected by unknown systematic effects such as the trend in eccentricities in Figure 21. The Monte-Carlo approach is also more time-efficient in the sense that it is independent of field size. The Jedicke and Metcalfe method requires a numerical integration over the entire field and becomes very slow for fields larger than about 5 degrees in size. To achieve the same resolution in orbital element space for a field twice the size as the original field requires doubling the number of integration steps, and this has the effect of squaring the running time for each factor of two increase in field size. Other advantages of the Monte-Carlo approach include the fact that varying the V magnitude efficiency does not require new runs of the main program (resulting in a factor of two increase in running time for each additional V efficiency to be tested), and the fact that the effect on the bias of different input orbital element distributions can easily be evaluated. Also of importance is the fact that the Monte-Carlo approach can be sped up dramatically by some simple changes in the program, such as generating the objects in a subroutine rather than reading them in from a file, as well as simple checks on M to see if the object can possibly be in the field. The Monte-Carlo approach is also, at present, the only acceptable method for debiasing high-inclination asteroid populations because of the strong dependence on

the angular orbital elements in the calculation of P. Because of these advantages, I recommend using this Monte-Carlo approach to debiasing future surveys.

2) Jedicke and Metcalfe's method, with a slight modification, was applied to the Palomar-Leiden asteroid survey, allowing debiased a, i, and H distributions to be computed. These results for total numbers in each main belt zone have been compared with those of Jedicke and Metcalfe on Spacewatch data and our results show systematically smaller numbers in each zone. Our method also makes possible the extraction of the the e distribution, something Jedicke and Metcalfe could not present adequately. Our results show that the slope of the absolute magnitude-frequency distribution is constant, to within the error bars, at a value of $\alpha = 0.45$. This can be translated into a mass index, q, of 1.75, which is slightly less than the canonical Dohnanyi value of 1.833 and Durda's (1995) value of 1.78. Our results also show that in the H range 13-15.5 the asteroid belt is dominated by the 4 main families of Eos, Themis, Koronis and Maria, and that they represent at least 1/5 of all of the asteroids in this H range. While there still appear to be some errors in the debiased PLS results from this study, it is recommended that until a properly debiased large-scale survey is undertaken researchers use the orbital element distribution presented here as the model asteroid population for the main belt. For the H distribution, Jedicke and Metcalfe's results are probably better simply because they had 10 times as many detections.

3) The Palomar-Leiden asteroid survey was deficient with regards to high-inclination asteroids, and thus we were forced to design and conduct our own survey for these bodies at high ecliptic latitudes. As these orbits tend to be correlated in the angular elements, we also were forced to abandon the Jedicke and Metcalfe method for debiasing and use TBS method. When applied to the BSS, this allowed the first-ever debiasing of the Hungaria and Phocaea asteroid populations. Because of small-number statistics, we used the maximum likelihood method for determining

α, the slope of the absolute magnitude-frequency distribution. These results show that α is again very near 0.45. This survey also resulted in a number of interesting discoveries, among them at least one new asteroid dynamical family, a new long-period comet, and the closest approaching significantly-sized NEO, 1996 JA_1.

7.2 Future Work

This work has allowed us to make some suggestions for the direction of future work in this field. First and foremost, it is hoped that this study will encourage future asteroid survey teams to consider debiasing when designing surveys, rather than simply conducting a survey purely for discovery. Second, and perhaps most important, is the clear need for a properly debiased large-scale survey. Because PLS covered too small an area of sky, and Spacewatch data do not contain good orbits, we still do not have good results for the debiased orbital element distribution, or faith in the results from the size distribution studies. Figure 38 is a composite of Jedicke and Metcalfe's Figure 5, and our Figure 28, and illustrates the problems we still have with regard to total numbers of asteroids. Note that, because of the problems discussed in Section 4.7, my PLS results are lower limits. The fact that this prediciton crosses the Jedicke and Metcalfe prediction at the faint end, yet severly underestimates the number of objects at the bright end, indicates that there are still some serious problems with the debiased results for the main asteroid belt. This large-scale survey must be debiased to much finer resolution than the 5 degree i bins and 0.05 AU a bins, and 0.5 magnitude H bins. These results would be valuable for determining precisely how many asteroids there are in the main families. This finer resolution would also prevent the loss of information on the structure of the asteroid belt that arises from using such large bins. Another important by-product of this type of survey would be the precise distribution of objects near resonances, and this could be used to discern the source of the NEO's. A small-scale, very faint survey would also provide much information on the size distribution of the smallest asteroids. Of vital importance to all of this work is not only properly determined V magnitudes, but also rotation periods, albedos, and formal radii for each object observed. The true size distribution cannot be obtained without the properly determined sizes themselves.

The Monte-Carlo technique is ideal for debiasing the NEA population, and the Short-Period Comet population, two studies that to date have not been attempted. The Trans-Neptunian population could also be debiased with this method. These results would be of great use to solar system research.

The TBS method will also permit debiasing in all 7 dimensions, something that to date cannot be achieved using the Jedicke and Metcalfe method. This true distribution of asteroid orbital elements in all dimensions would allow for many opportunities to study the dynamics of the asteroid belt, with specific attention being paid to resonances, NEA sources, and the early solar system.

Directed surveys may be undertaken in the near future. Since much information on collisional studies must come from α for specific families, one could do a wide-field directed survey for the main families. Once the H and size distribution is determined to a specified limit, collisional researchers will be able to fine tune their models, and perhaps answer the age-old question as to whether asteroids are monolithic, or “rubble piles”.

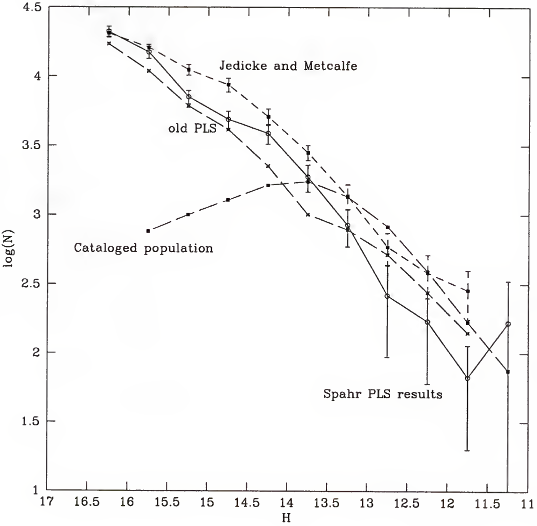

Figure 38. Comparison of predicted numbers of asteroids in zone 1 of the main belt (a = 2-2.6 AU) with the cataloged population.

REFERENCES

[1] Bowell, E., Chernykh, N. S., and Marsden, B. G. 1989. Discovery and Follow up of Asteroids. In *Asteroids II*, (R. P. Binzel, T. Genrels, and M. S. Matthews, Eds.) pp. 21-38. University of Arizona, Tucson.

[2] Brouwer, D. and Clemence, G. 1961. *Methods of Celestial Mechanics*, Academic Press, New York.

[3] Carusi *et al.* 1994. Carus, A., Gehrels, T., Helin, E. F., Marsden, B. G., Russell, K. S. , Shoemaker, C. S., Shoemaker, E. M., and Steel, D. I. 1994. Near-Earth Objects: Present Search Programs. In *Hazards Due to Asteroids and Comets* (T. Gehrels, Ed.), pp. 127-148. Univ. Arizona Press, Tucson.

[4] Dohnanyi, J. S. 1969. Collisional Model of Asteroids and Their Debris. *J. Geophys. Res.*, **74**, 2531-2554.

[5] Durda, D. D. 1993. Ph. D. Thesis.

[6] Durda, D. D. and Dermott, S. F., 1997. The Collisional Evolution of the Asteroid Belt and its Contribution to the Zodiacal cloud. *Icarus*, **130**, 1, p 140-164.

[7] Durda, D. D., Greenberg, R. and Jedicke, R. 1998. *Icarus* under review.

[8] Everhart, E. 1984. Finding Your Telescope's Magnitude Limit. *Sky and Telescope*, **67**, 28-32.

[9] Froeschle, Ch., and Scholl, H. 1989. The Three Principal Secular Resonances nu(5), nu(6), and nu(16) in the Asteroid Belt. *Cel. Mech. and Dynam. Astron.*, **46**, 3, p. 231-251.

[10] Gradie, J. C., Chapman, C. R., and Williams, J. G. 1979. Familes of Minor Planets. In *Asteroids*, Tucson, University of Arizona Press, pp. 359-390

[11] Hergenrother, C. W., Larson, S. M., and Spahr, T. B. 1996. The Hansa Family: A New High-Inclination Asteroid Family. *Bull. American Astron. Soc.*, DPS meeting **28, 10.07**.

[12] Hirayama, K. 1918. Groups of Asteroids Probably of Common Origin. *Astron. J.*, **31**, 185-743.

[13] Jedicke, R. 1996. Detection of Near-Earth Asteroids Based Upon Their Rates of Motion. *Astronomical Journal*, **111**, 970-982.

[14] Jedicke, R. and Herron J. D., 1997. Observational Constraints on the Centaur Population. *Icarus*, **127**, 2, 494-507.

[15] Jedicke, R. and Metcalfe, T. S. 1998 The Orbital and Absolute Magnitude Distribution of Main Belt Asteroids. *Icarus*, in press.

[16] Kirkwood, D. 1867. Meteoric Astronomy.

[17] Kresa'k, L. and Klacka, J. 1989. Selection Effects of Asteroid Discoveries and Their Consequences. *Icarus*, **78**, 287-297.

[18] Kuiper, G. P, Fujita, Y, Gehrels, T, Groeneveld, I, Kent, J, Van Biesbroeck, G and Van Houten, C. J. 1958. Survey of Asteroids. *Astrophys. J. Suppl.*, **3**, 289-428.

[19] Levison, H. F. and Duncan, M. J., 1994. The Long-Term Dynamical Behavior of Short-Period Comets. *Icarus*, **108**, 1, 18-36.

[20] Michel, P. 1997. Secular Resonances in the Inner Solar System. . *Icarus*, **129**, 2, 348-366.

[21] Mikkola, S. and Innanen, K. 1994. On the Stability of Martian Trojans. *Astron. J.*, **107**, 5, 1879-1884.

[22] Schmadel, L. D., Schubart, J., Schuster, H. E., and West, R. M. 1979. A Survey For High-Inclination Minor Planets. *Astronomy and Astrophysics*, **76**, 130-131.

[23] Shoemaker, E. M., Shoemaker, C. S., and Wolfe, R. S. 1989. Trojan Asteroids: Populations, Dynamical Structure and Origin of L4 and L5 Swarms. In *Asteroids II*, pp. 487-523, University of Arizona press, Tucson.

[24] Valsecchi, G. B, Carusi, A., Knezevic, Z., Kresak, L. and Williams, J. G. 1989. Identification of Asteroid Dynamical Families. In *Asteroids II*, pp. 368-385, University of Arizona Press, Tucson.

[25] Van Houten, C. J., Van Houten-Groeneveld, Herget, P., and Gehrels, T. 1970. The Palomar-Leiden Survey of Faint Minor Planets. *Astr. Astrophys. J. Suppl.*, **2**, 339-448.

[26] Wisdom, J. 1982. The Origin of the Kirkwood Gaps - A Mapping for Asteroidal Motion Near the 3/1 Commensurability. *Astron. J.*, **87**, 577-593.

[27] Wisdom, J. 1983. Chaotic Behavior and the Origin of the 3/1 Kirkwood Gap. *Icarus*, **56**, 51-74.

[28] Wisdom, J. 1985. Meteorites May Follow a Chaotic Route to the Earth. *Nature*, **315**, 731-733.

BIOGRAPHICAL SKETCH

Timothy B. Spahr was born in Xenia, Ohio on April 7, 1970. At age 6, he saw Comet West and was forever in love with astronomy and planetary science. After graduation from Fairborn High School in 1988, he attended the University of Arizona, obtaining a BS in physics and astronomy in 1992. Tim will receive his doctorate in May 1998.

I certify that I have read this study and that in my opinion it conforms to acceptable standards of scholarly presentation and is fully adequate, in scope and quality, as a dissertation for the degree of Doctor of Philosophy.

Stanley Dermott , Chairman
Professor of Astronomy

I certify that I have read this study and that in my opinion it conforms to acceptable standards of scholarly presentation and is fully adequate, in scope and quality, as a dissertation for the degree of Doctor of Philosophy.

Henry E. Kandrup
Professor of Physics and Astronomy

I certify that I have read this study and that in my opinion it conforms to acceptable standards of scholarly presentation and is fully adequate, in scope and quality, as a dissertation for the degree of Doctor of Philosophy.

Charles M. Telesco
Professor of Astronomy

I certify that I have read this study and that in my opinion it conforms to acceptable standards of scholarly presentation and is fully adequate, in scope and quality, as a dissertation for the degree of Doctor of Philosophy.

Haywood C. Smith Jr

Haywood C. Smith, Jr.
Associate Professor of Astronomy

I certify that I have read this study and that in my opinion it conforms to acceptable standards of scholarly presentation and is fully adequate, in scope and quality, as a dissertation for the degree of Doctor of Philosophy.

Paul Mueller
Professor of Geology

I certify that I have read this study and that in my opinion it conforms to acceptable standards of scholarly presentation and is fully adequate, in scope and quality, as a dissertation for the degree of Doctor of Philosophy.

Humberto Campins
Professor of Astronomy

This dissertation was submitted to the Graduate Faculty of the Department of Astronomy in the College of Liberal Arts and Sciences and to the Graduate School and was accepted as partial fulfillment of the requirements for the degree of Doctor of Philosophy.

May 1998

Dean, Graduate School